Waseda University

Doctoral Dissertation

Studies on Estimation of Water Content Ration in Cylindrical-Shaped Objects Using Radar-Cross-Section

レーダー・クロス・セクションを用いた円柱形状物質内の
水分量推定に関する研究

February 2018

Graduate School of Global Information and
Telecommunication Studies

Media Art Research II

Fahad Saleh A Algneaer

1. ACKNOWLEDGMENTS

I am greatly indebted to the many people who have helped me accomplish this work. First and foremost, I would like to express my sincere gratitude to my supervisor, Prof. Shigekazu Sakai, and his team. This work could not have been completed without the tremendous help from the faculty members of the Global Information and Telecommunication Studies department at Waseda University during studies for my PhD.

I would also like to convey my special thanks to Prof. Takuro Sato and Prof. Shigeru Shimamoto for my doctoral thesis review and supervision. I am grateful for their willingness to be reviewers and judges of my doctoral thesis, as well as for their helpful, constructive advice.

I wish to express special thanks to Alouette Technology Corporation, represented by Mr. Nohmi and his staff, for allowing the use of his radar equipment and for his guidance during the experiments. I would also like to thank my parents and family for their continuous encouragement and support during my studies. Finally, thank you to the many friends I have met during my studies at Waseda University, especially Abdullah Alshehab, Ahmed Bingyth and Mohammed Almogbel, for their support and encouragement. They made this experience a more pleasant one.

This project was funded by my sponsor, King Abdulaziz City for Science and Technology (KACST), Riyadh, Saudi Arabia.

2. TABLE OF CONTENTS

3. LIST OF FIGURES

4. LIST OF TABLES

SUMMARY

Nowadays, the use of remote sensing in applications to detect and monitor changes in the global environment is being promoted as a means of resolving problems in many fields such as agriculture, forestry, and civil engineering. In particular, the author's ultimate aim is to contribute to detection and monitoring processes that minimize damage inflicted on the agricultural industry specially for date palm trees in the Middle East.

In the Middle East, the date palm tree is considered the most important species, both agriculturally and economically. However, during the past few decades, the date palm tree has faced risks in terms of survival following the infestation of an insect, the red palm weevil. These insects bore into the trunk, damaging the tree and ultimately causing it to die.

Microwaves can be used to remotely monitor various types of vegetation, and thus to non-invasively determine conditions without harming the object being measured. Therefore, in this dissertation, we proposed the use of three RCS measurement systems developed specifically for the purpose of this study. Each system was equipped with different frequency band (L, X and Ku bands), the three frequency bands chosen are those most commonly used for remote sensing.

Two experiments are carried out using the developed RCS measurement systems that are applied to prove that microwave backscattering can be utilized to remotely measure the water content in objects (specifically, palm trees) and, thus, determine changing conditions in terms of tree health.

Issues addressed during experimentation included the methods used to measure and evaluate microwave backscattering intensity, and the information that can be obtained about an object through the analysis of microwave backscattering measurements alone.

In the first experiment, our goal was to measure the water content inside cylindrical-shaped objects made of phenolic foam material with different water content levels using only microwave backscattering.

The experiment was carried out in an anechoic chamber using RCS measurement systems three frequency bands: L, X, and Ku. Four objects with a different volume of water permeating were irradiated by microwaves, and the backscattering was measured. The columns were placed on a turntable and rotated one revolution (i.e., 360º) while taking about 75,000 continuous measurements of the entire surface. The measurements were then evaluated based on variance and median of the calculated radar cross-section (RCS) values. As a result of measuring the microwave backscattering, it was found that the higher the water content in the column, the higher the RCS median, average, and maximum values for that object in all three bands.

The second experiment, which expands on the successful first experiment explained, replacing the cylindrical-shaped objects with actual palm tree trunks (Sago palm) and periodically irradiating the tree trunks over a set timespan to determine whether changes in the trunks' condition can be monitored by analyzing the intensity of the microwaves backscattered off them. The goal of this experiment is to confirm whether or not changes that occur in tree trunks over a period of time due to some influence can be measured remotely using microwave backscattering. If it is proven that this is possible, the changing state of trees can be monitored remotely, doing so non-invasively without causing physical damage or harm to the trees. The results of the L band measurements suggest interesting possibilities. Irradiating microwaves in the L band or lower frequencies, it was shown that change inside an object, even a thick-barked tree like the Sago palm tree used in this experiment, can be determined.

This dissertation is presented in six chapters. Chapter 1 begins by explaining the importance of measuring the water content in vegetation such as plants and trees, describing the fundamental principle of electromagnetic waves (microwaves) and the ways in which these waves can be applied to measure water content in objects, and expanding the application of microwaves in various fields, such as the remote sensing of water content in vegetation. Chapter 2 explains the methods for utilizing microwaves to measure water content. The chapter discusses the traditional method, proposes a new methodology utilizing microwave backscattering, and provides an explanation of microwave backscattering. Chapter 3 discusses conventional devices and systems utilized to measure water content, including the transmissivity water content meter, the weather radar, ultra-wide-band radar (UWB), vector network analyzers (VNAs) and the proposed developed system (i.e., the RCS measurement system) for enabling measurements in the field sometime in the future. The chapter explains the RCS measurement system structure, measurement mechanism and processes, and advanced features that make it unique as compared to other devices. Chapter 4 presents the first experiment, which focuses on measuring the water content in cylindrical-shaped objects made of a foam material. Chapter 5 presents the second experiment, which expands on the experiment explained in Chapter 4, replacing the cylindrical-shaped objects with actual palm tree trunks and periodically irradiating the tree trunks over a set timespan to determine whether changes in the trunks' condition can be monitored by analyzing the intensity of the microwaves backscattered off them. Chapter 6 discusses and concludes the findings, and explains plans for future work.

CHAPTER 1 – INTRODUCTION

1-1 The Importance of Measuring Water Content in Vegetation Such as Plants and Trees

The amount of attention that global warming receives has grown dramatically throughout the world. In parallel to this, but not reported as extensively, are increasingly serious problems with the Earth's ecosystem—ecological abnormalities that are just as important because they affect the micro-ecosystems of plant and animal life. Changes in ecosystems and regional climates believed to be caused by global warming and environmental pollution are key topics of discussion around the world. In Europe, it has been reported that flowering, leaf development and the fruition time of vegetation have abnormally quickened in 78% of 542 species of plants in the past 30 years (i.e., from 1971 to 2000) [1]. In China, the number of bamboo trees—the panda's main source of food—has drastically decreased, and the possibility of the extinction of wild pandas has become a major concern [2]. In Africa, the Sahara Desert continues expanding southward, with 1.5 million hectares of land moving towards desertification per year [3]. Economically weak and developing countries tend to suffer the most from environmental change, which leaves them susceptible to food shortages and agricultural damage resulting from droughts, floods, and other extreme conditions.

In the Middle East, the date palm tree (*Phoenix dactylifera*) is considered the most important species, both agriculturally and economically. The fruit that the tree produces is a highly valued and sought-after agricultural product, and has been a primary source of food in Middle Eastern countries for centuries [4].

However, during the past few decades, the date palm tree has faced risks in terms of survival following the infestation of an insect, the red palm weevil (*Rhynchophorus ferrugineus*) (Fig.1-1). These insects bore into the trunk, where they lay their eggs. After the larvae hatch, they feed on the soft, wet internal wood, damaging the tree and

ultimately causing it to die [5]. Adult red palm weevils can fly tens of kilometers, allowing the insect to infest palm trees on farms throughout the region. It has been reported that infestation by the insect is expanding across many areas, including Eastern Asian countries [6][7].

Figure 1-1 Red palm weevils at different life stages.

Date palm tree farms in the Middle East are found primarily in arid areas. A healthy date palm stores a larger volume of water in its trunk than do other trees in the region. However, because the date palm tree's outer bark is characteristically very dry in appearance and touch, it is difficult to detect the moisture content and health of the tree by visual inspection.

Saving infested trees is possible if the insects' presence is discovered in its early stages. However, finding the insects at an early stage is difficult because the damage they inflict upon the tree is internal and appears only during a later stage of infestation.

Another issue is that the farm areas used for growing date palm trees are widespread, making it virtually impossible to inspect the trees one by one for infestation. Therefore, an efficient process to check tree health is needed [8].

In organisms such as plants and animals, fluctuations in internal water content significantly affect life support. In humans, approximately 60% of the adult body is water; if this amount reduces by 5%, the result can be reactions such as heat stroke [9]. For fresh foods such as fruits and vegetables, the amount of water contained significantly affect taste and quality [10]. In addition, decreased water content in a tree trunk is regarded as an indication of internal erosion caused by the infestation of microorganisms or insects, or by the invasion of small animals. In the study of natural disasters, research has shown that underground water content and soil saturation can induce avalanches and landslides, and the resulting destructive power is related to internal water content [11]. The possibility of measuring water content—or its changes—in an object will create a different solution for such issues in agriculture fields.

Hypothetically, if it is possible to closely monitor regional ecosystems in a way that helps prevent the loss of agricultural crops, the result could help reduce the economic and food shortage problems that result from global warming and other climatic changes.

1-2 Using Electromagnetic Radiation to Measure Water Content

Various methods exist to monitor the health conditions of living organisms. These methods differ depending on the characteristics of the organism being monitored. In the case of vegetation, good indicators are the leaf's visual appearance and the amount of water it holds internally[12]. For example, monitoring the water content of

fruits and vegetables is a useful way to determine a crop's maturity, while monitoring the internal moisture of grains has proven beneficial in managing grain storage and preserving taste[13]. In the case of tropical evergreens and palm trees, the change in water content in the tree trunk is a good indicator of tree health.

Electromagnetic radiation (i.e., microwaves) behaves in a specific manner based on wave theory. Essentially, microwaves form a pulsating electric field that varies in magnitude, moving perpendicular to the direction in which the microwaves are traveling and a magnetic field oriented at right angles to that electric field. Additionally, microwaves maintain two characteristics that are particularly important for understanding their use in extracting information from remote sensing data: wavelength and frequency (Fig. 1-2). Wavelength is the length of one wave cycle, measured as the distance between successive wave crests. Frequency is the number of cycles of a wave passing a fixed point per unit of time. These two characteristics are related using Maxwell's wave theory formula (Eq. 1-1),

$$c = \lambda\nu \quad \text{(Eq. 1-1)}$$

where λ is the wavelength in meters, ν is the frequency in hertz and c is the speed of light. Therefore, the two are inversely related to each other: the shorter the wavelength, the higher the frequency, and the longer the wavelength, the lower the frequency.

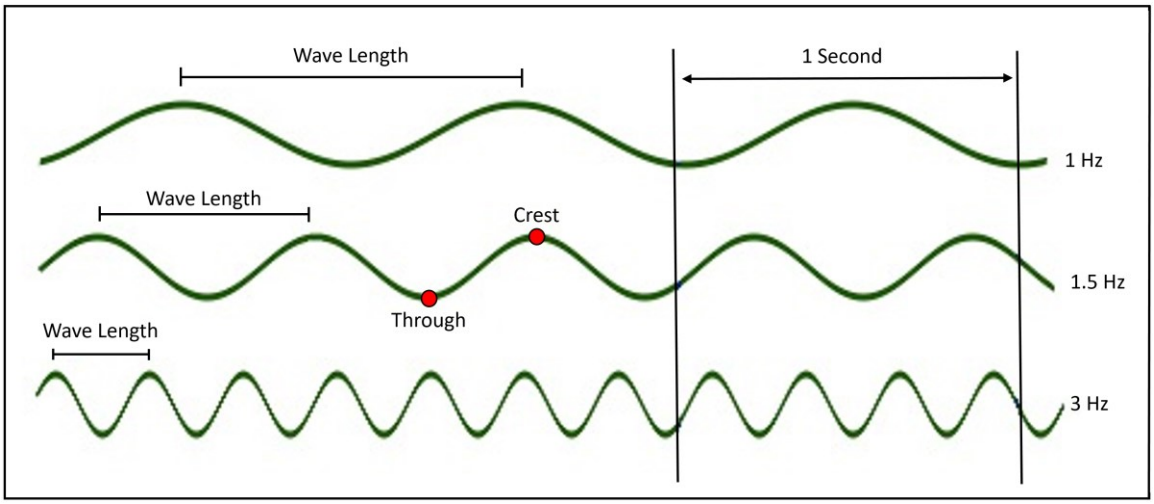

Figure 1-2 Wavelength and frequency of microwaves.

"Microwaves" refers to the electromagnetic radiation of frequencies ranging from approximately 300 MHz to 300 GHz. Microwaves have been applied in various ways depending on the frequency range. Lower frequencies offer a significant advantage in the measurement of soil and vegetation moisture; the difference in frequency used leads to a significant difference in the vegetation penetration capability (Fig. 1-3).

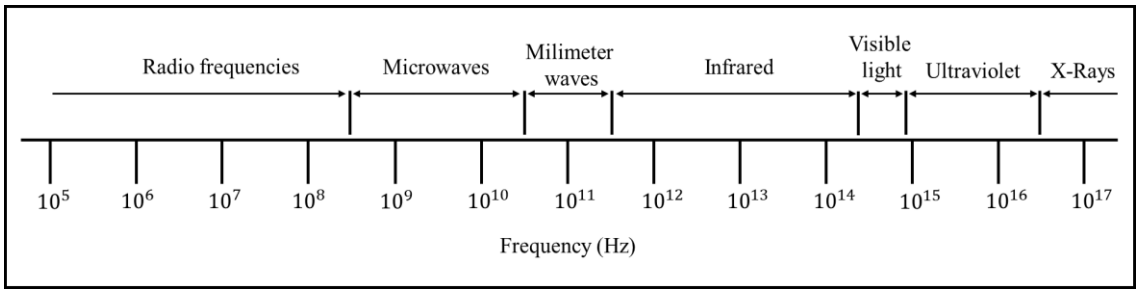

Figure 1-3 Electromagnetic spectrum.

Applying the abovementioned principle, and considering their characteristics, microwaves are used to measure objects' water content in various fields. In terms of socio-economic improvements, the use of microwaves to monitor and measure applications has been extremely beneficial, especially in the areas of forestry, agriculture and civil engineering. Examples of such water resource management include monitoring precipitation [14], measuring and monitoring soil moisture content

[15][16], and managing vegetation, such as monitoring deforestation [17] and desertification [18]. In addition, meteorological stations around the world use microwaves to inform regions about inclement weather.

The number of applications for monitoring vegetation is increasing, but as with soil moisture applications, most vegetation applications cover vast areas, and limited development has been achieved in terms of monitoring the status/conditions of plants individually. It is also known that information about the water content in vegetation is vital for monitoring plant health and growth status, and that such information can be used for early detection of the presence of disease and/or the infestation of harmful insects. For example, the presence of certain insects—such as the red palm weevil, which feeds on and harms date palm trees by tunneling through their internal tissue—in or on plants is directly related to the amount of water in the tree [19].

Agri-food moisture measurement applications have become an essential means of ensuring food quality; such measurements are achieved using various techniques [20][21]. However, these measurements are carried out mainly in factories and laboratories, and require sensors connected to moisture meters or specially manufactured devices [22]. Even so, based on the abovementioned applications, it is believed that the measurement of water content using microwaves is, in general, advantageous.

1-3 New Technologies and Broadening Practical Applications

A high possibility exists of a dramatic future expansion in the practical application of microwaves in various areas in the future. The driving force behind this expansion is the rapid advancement in related technological areas in recent years—for example, the evolution of mobile telephone technologies and the ongoing application of radar

in the automobile industry and transportation infrastructure. As a result, the features of massive and bulky radar equipment applied several years ago in large-scale, high-cost systems mounted in satellites and large aircraft are now becoming available in much smaller-sized systems that can be obtained at affordable prices. This makes them attractive for lower-budget projects. For example, private enterprises can now relatively easily obtain synthetic aperture radar (SAR) equipment and components at a lower price.

Evolutionary improvements have also been made in the design tools for microwave-related electronic circuits and antennas. These tools are now readily available. Device development that once required repeated trial and error and daunting calculations during the design phase is now simulated using computers and simulation tools, making tasks easier to implement and complete, and doing so at a much lower cost.

Several types of microwave measuring devices are now available, and their cost is much more reasonable. As a result, the investment risk for system development is decreasing. Accordingly, several small companies are now developing microwave-related equipment. One example is the transmission-type microwave moisture meter [23], which uses microwave transmission and reception to take measurements. The energy of the microwaves passing through the water molecules inside an object is consumed, and the transmitted energy is attenuated. After this, the amount of moisture inside the object can be calculated based on the amount of attenuated microwaves. This device is currently utilized to measure residual moisture in various substances such as lumber for construction, and earth and sand sediments. It is also used to measure the water content of foodstuffs and chemicals [24].

We believe that if we can measure the water content inside the solid by utilizing state-of-the-art technology, we can obtain greater merit than ever in solving

environmental problems, especially in vegetation related issues. Therefore, this dissertation summarizes the results of a new challenge to utilize our proposed technology in the field of remote sensing to measure the water content inside the targeted objects.

1-4 Thesis Structure

This thesis and the supporting content herein are derived from the author's sincere interest in developing a methodology for expanding the use of microwave technologies in the agriculture/farming industry. Witnessing the destructiveness of the red palm weevil in the Middle Eastern date industry became the driving force behind the author's focus on this subject matter. The goal is to successfully deliver technologies and/or products that support the realization of a better life for all.

The remainder of this dissertation is presented as follows. Chapter 2 explains the basic principles behind methods that utilize microwaves to measure water content. The chapter discusses the traditional method and proposes a new methodology; the former is based on the use of the dielectric constant to determine water content, while the latter is based on the use of the measurement and evaluation of microwave backscattering intensity to determine water content. The chapter also includes an explanation of microwave backscattering.

Chapter 3 discusses conventional devices and systems used to measure water content, including the transmissivity water content meter, the weather radar, ultra-wide-band radar (UWB), vector network analyzers (VNAs), and the proposed developed system (i.e., the RCS measurement system) for enabling measurements in the field sometime in the future. The chapter also explains the device structure, the measurement

mechanism and processes, and the advanced features that make it unique compared to other devices.

Chapter 4 presents the first experiment, which focuses on measuring the water content in cylindrical-shaped objects made of a foam material. Our goal was to measure the water content inside phenolic foam columns using only microwave backscattering measurements by using a RCS measurement system developed for airborne synthetic aperture radar (SAR). The experiment was carried out in an anechoic chamber using RCS measurement systems three frequency bands: L, X, and Ku. The column irradiated with microwaves was a cylinder of phenolic foam capable of holding various volumes of water. Four objects with a different volume of water permeating were irradiated by microwaves, and the backscattering was measured. In consideration of the influence of microwave fading, the columns were placed on a turntable and rotated one revolution (i.e., 360º) while taking about 75,000 continuous measurements of the entire surface. The measurements were then evaluated based on variance and median of the calculated radar cross-section (RCS) values. As a result of measuring the microwave backscattering, it was found that the higher the water content in the column, the higher the RCS median, average, and maximum values for that object in all three bands. Regarding the L band, it was clearly shown that it was possible to distinguish when the volume content of water was 25% and 50%. Also, when the water content of the column was relatively small, the range of dispersion was large, and when the water content exceeded a certain value, the dispersion widths began to converge. This indicates the possibility that analyzing the variance of the microwave backscattering may be a clue to knowing the dispersion state of the water content of the object. In this experiment, the microwave backscattering was

continuously measured while rotating the object one time, and a statistical method was used to analyze the results.

Chapter 5 presents the second experiment, which expands on the experiment explained in Chapter 4, replacing the cylindrical-shaped objects with actual palm tree trunks and periodically irradiating the tree trunks over a set timespan to determine whether changes in the trunks' condition can be monitored by analyzing the intensity of the microwaves backscattered off them. The goal of this experiment is to confirm whether or not changes that occur in tree trunks over a period of time due to some influence can be measured remotely using microwave backscattering. If it is proven that this is possible, the changing state of trees can be monitored remotely, doing so non-invasively without causing physical damage or harm to the trees. The results of the L band measurements suggest interesting possibilities. Irradiating microwaves in the L band or lower frequencies, it was shown that change inside an object, even a thick-barked tree like the Sago palm tree used in this experiment, can be determined.

Chapter 6 presents the author's discussion and conclusions, and explains plans for future work.

CHAPTER 2 - METHODS FOR MEASURING WATER CONTENT UTILIZING MICROWAVES

2-1Measurement Target and Method

There are two major methods utilizes microwave to determine water content, by measuring the dielectric constant of an object, and by utilizing the microwave backscattering.

Various applications measure the dielectric constant to determine the water content in materials. For example, in food materials such as wheat, grains, and building materials such as bricks, concrete, and timbers [25][26].

An example for the microwave backscattering methods is the applications of soil moisture and vegetation cover measurements using satellites or aircraft equipped with synthetic aperture radar (SAR) or scatterometers that take measurements using different frequency bands, such as L-, X- and Ku-bands [27][28][29].

Ulaby and Dobson conducted extensive studies of terrain using microwave backscattering methodology, and collected hundreds of thousands of data points derived from measurements using both airborne and ground-based scatterometer systems. They compiled those data points into tables and a database, which other researchers have referenced. This information has been used as a standard not only for calibration and measurement accuracy, but also for detailed category identification. In addition, the measurement results have been analyzed using statistical methods, and are considered a reliable information source. Here, the relationship between various objects, such as rocky soil, vegetation, snow, ice and artifacts (city), and microwave backscattering is shown as a distribution chart, along with theoretical considerations [30].

The methods for utilizing dielectric constant and microwave backscattering will be explained in detail in the next section.

2-2Utilizing Dielectric Constant

One of the most-used techniques for estimating water content is measuring an object's dielectric properties. The dielectric constant is the measurement of an object's ability to store an electrical charge; the loss factor is the measurement of the electromagnetic field energy (oscillation) that microwaves in the object generate. When microwaves irradiate a given object, a change occurs in the distribution of that object's molecular charges. The resulting measurement of the charge distribution in the object is known as the object's "dielectric permittivity." The expression of dielectric permittivity in relation to free space is the "relative permittivity." Relative permittivity is related to the dielectric constant and loss factor, as shown by (Eq. 2-1):

$$E_r = E_r' - JE_r'' \quad \text{(Eq. 2-1)}$$

where, E_r is the relative permittivity, E_r' is the dielectric constant and JE_r'' represents the loss factor [31].

Two methods exist to measure an object's dielectric properties: invasive and non-invasive [32]. The invasive method requires that sensors (e.g., a metal rod or probe) be inserted into the object to measure the dielectric properties (Fig. 2-1 A). Therefore, this method creates the problem of damaging the object. The non-invasive method requires placing the object between two antennas to measure the dielectric properties (Fig. 2-1 B). This is referred to as the "free-space method". During the measurement process, the sensors/antennas are commonly connected to a VNA [33][34][35].

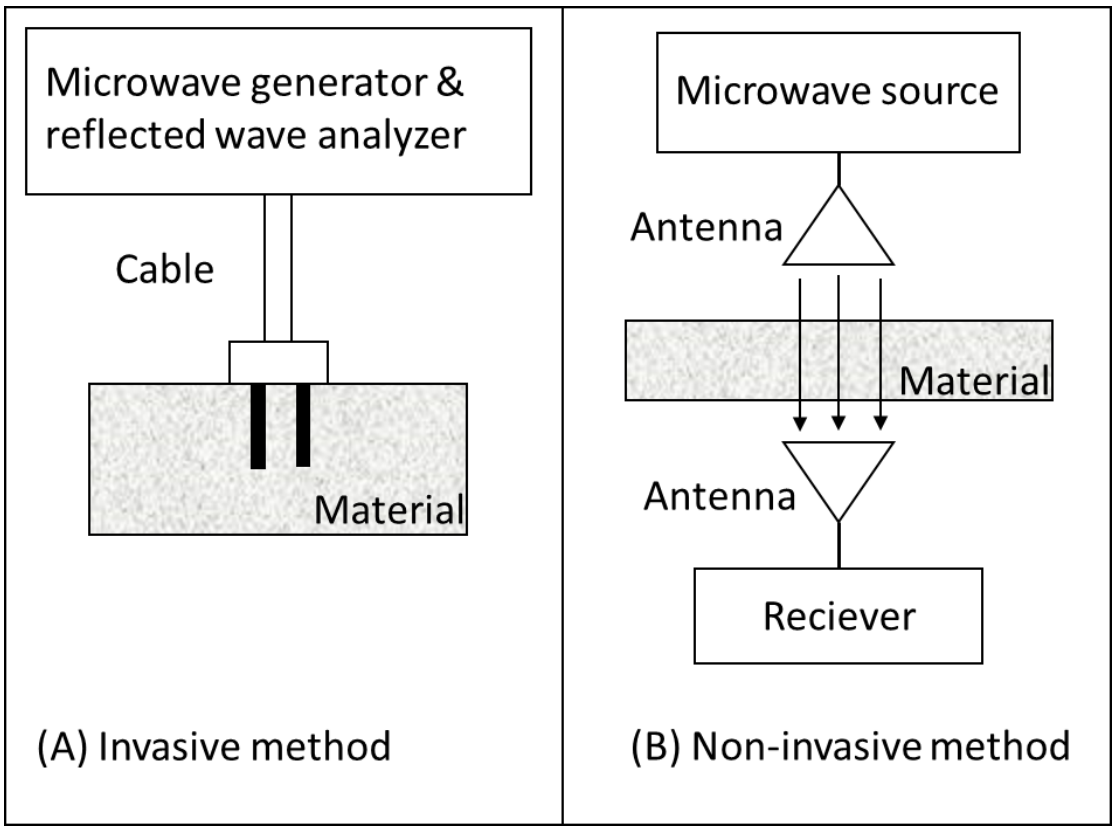

Figure 2-1 Dielectric properties measurement methods.

Various studies have compared the accuracy of measuring the dielectric constant against that of a microwave backscattering analysis, and evidence exists that the use of the dielectric constant measurement is more accurate. For example, a study concluded that backscattering analysis, while having an exponential relationship to the dielectric constant, is not as accurate, as it overestimated the soil content [36][37][38].

Even so, while the invasive measurement of dielectric constant is more accurate and requires less computational time, this measurement method cannot be used to meet this study's objectives, as it requires direct contact with the object being measured.

Additionally, while the non-invasive method has succeeded at measuring the water content in various objects, for example, using it to measure the water content in foods, wood and other products in a manufacturing setting, the need to have antennas on

opposite sides of the object being measured is not appropriate for this study's objectives.

Another issue that could arise includes random error due to noise, drift and/or environmental factors such as temperature, humidity, and barometric pressure, which cannot be accounted for in measurement calibrations. This leaves the data susceptible to error due to small fluctuations in conditions at the time of measurement.

Finally, while VNAs are commonly used to gather data during dielectric property analysis, as stated above, VNA operational specifications are not sufficient to enable their use in gathering the microwave backscattered data required for measuring the water content in remote objects.

2-3 Utilizing Microwave Backscattering

By definition, microwave backscattering is "the scattering of electromagnetic field radiation (microwaves) in a direction opposite to that of the incident direction of travel caused by reflecting off of the bipolar molecular structures in the object the microwaves are passing through". Water is one such bipolar molecular structure. Therefore, when microwaves penetrate an object in the incident direction of radiation, and when that object contains water, the microwaves are reflected. Accordingly, the theory proposed herein is that microwave backscattering can be used as a non-invasive remote sensing method capable of detecting the water content in objects irradiated by microwaves by measuring the microwave backscattering intensity. However, merely recording the intensity of the microwaves backscattered from an object does not reveal the water content. A method of analyzing and evaluating the intensity measurements obtained is also required.

2-3.1 Theoretical model of microwave backscatter and reflection

Backscatter is a diffuse reflection scattered in all directions after microwaves contact an object's surface. The size of the scattered particles is often parameterized by the ratio x (Eq. 2-2):

$$x = \frac{2\pi r}{\lambda} \quad \text{(Eq. 2-2)}$$

where r is the characteristic length (radius) and λ is the microwave wavelength. This wavelength dependency is characteristic of dipole scattering, and volume dependence applies to all scattering mechanisms.

When the object presents $x \gg 1$, scattering is geometric in shape. With Mie scattering, when x is an intermediate ($x \simeq 1$), phase variations caused by the object's surface generate interference. Here, the water droplet diameter is equivalent to the size of the optical refraction and will increase along with increased diffraction in the direction of wave travel. This results in weaker backscatter.

In the case of Rayleigh scattering, which is the microwave theory applied in weather radar to measure the reflection off raindrops in clouds, the scattered particles are very small, $x \ll 1$, less than one-tenth the size of the wavelength. Accordingly, the entire surface radiates the same phase. In other words, if the wavelength is larger than the raindrop's diameter, the measured backscatter is proportionate to the object's ability (power) to reflect the microwave times the object's reflection properties to the power of six [39].

The microwave vertical reflectance for a dielectric medium such as water is expressed by (Eq. 2-3):

$$\gamma = \frac{\sqrt{\varepsilon}-1}{\sqrt{\varepsilon}+1} \quad \text{(Eq. 2-3)}$$

where ε is the dielectric constant. Therefore, the reflectance depends on the dielectric constant. As the microwave frequency increases, the dielectric constant decreases due to the "dipolar polarization effect," so vertical reflectance decreases as the frequency increases [40].

2-3.2 Applying radar cross-section (RCS) values to measure water content

When a radar signal is incident on a target, one of the most important parameters for detection is the amount of energy reflected (i.e., backscattered). The measure of the target's 'size' is called its radar cross-section (RCS)[41]. An object's RCS value is defined as the effective area intercepting an amount of incident power which, when scattered isotopically, produces a level of reflected power at the receiver (antenna) equal to that from the object. The following equation is used to calculate the RCS (Eq. 2-4):

$$RCS = \frac{S_R(4\pi)^3 R^4}{A.G_T.G_R.\lambda^2} \quad \text{(Eq. 2-4)}$$

where S_R is the received power, A is the receiver gain, G is the antenna gain, R is the distance between the antenna and the object, and λ is the radar's wavelength.

The backscattering coefficient depends highly on the scattering mechanism involved. Scattering mechanisms can be classified into surface and volume scattering [42]. The amount of energy reflected due to surface scattering depends on the surface roughness, wavelength and angle of incidence. The smoother the surface, the less power is backscattered because the surface behaves like a mirror. Volume scattering occurs when the microwaves penetrate an object's surface. The penetration depth depends on

the microwave wavelength and the object's surface characteristics. It increases with higher wavelengths and decreases as the object's water content increases [43].

One of the objectives of this study was to obtain the RCS values for the entire surface of the objects being measured and to analyze those values to determine the characteristics including water content of each object. For Experiment 2 (Chapter 5), RCS values for each palm tree trunk measured were obtained at different times over a period of approximately three months, and were analyzed to determine the tree trunks' conditions. This required calibrating the systems before taking the actual palm tree trunk measurements and incorporating the calibration values as reference data when calculating the RCS after taking all the measurements.

2-3.3 Calibration for data measurement

In measurements using radar, determining the non-inductivity, mass and volume of an object is impossible. However, it is possible to calculate the reflection intensity from the relative reflection intensity using radar cross-section (RCS) values.

A theoretical RCS value is calculated using (Eq. 2-5), where L is the corner reflector diameter utilized for calibration, and λ is the microwave's wavelength.

$$\frac{12\,\pi L^4}{\lambda^2} \quad \text{(Eq. 2-5)}$$

To calculate the RCS for each object measured, the value of the receiver gain (A) must be found to determine the RCS for the data that each scatterometer measured. This is done using (Eq. 2-6), where RCS denotes the theoretical RCS value, S_R is the energy measured during calibration, G_T is the transmitter antenna gain, G_R is the receiver antenna gain and R is the distance from the column.

$$A = \frac{S_R(4\pi)^3 R^4}{G_T.G_R.\lambda^2.RCS} \quad \text{(Eq. 2-6)}$$

After finding the value of A, the value of RCS is calculated for each column measured using (Eq. 2-7).

$$RCS = \frac{S_R(4\pi)^3 R^4}{A.G_T.G_R.\lambda^2} \quad \text{(Eq. 2-7)}$$

CHAPTER 3 – CONVENTIONAL SYSTEMS AND THE PROPOSED SYSTEM FOR MEASURING WATER CONTENT IN OBJECTS

3-1 Conventional Devices/Systems and Related Problems

Several devices utilize microwaves to measure objects' water content. This section discusses several conventional devices/systems.

[Transmissivity water content meter]

Transmissivity water content meters use the transmission and reception of microwaves to take measurements. The energy of the microwaves that come in contact with water molecules inside an object is consumed, the transmitted energy is attenuated, and the amount of moisture inside the object is calculated based on the amount of attenuated microwaves. Therefore, if the conditions of the object and its surrounding environment are appropriate, the accurate measurement of moisture content as an order of percent (weight ratio) is possible. This method is currently used to measure residual moisture in various substances, such as lumber for construction, and earth and sand sediments. The method is also used to measure the water content of foodstuffs and chemicals [32].

However, though transmissivity water content meters can measure the water in an object without physical contact, some restrictions exist with respect to its practical use. The fact that the object to be measured must be placed between two opposing antennas limits the size, shape and location of the objects that can be measured. Furthermore, taking such a device into the field to measure the water content of objects existing in nature is difficult. Therefore, the use of transmissivity water content meters is not appropriate for achieving the author's objectives.

[VNAs]

VNAs were introduced in the 1980s for use in radio frequency (RF) metrology, including microwave measurements and the development and manufacture of avionic and radar components; that is, they measure the incident, reflection, and transmission of electromagnetic energy in electrical devices and networks. Essentially, network analysis focuses on the accurate measurement of the ratio of reflected signal to incident signal and the ratio of transmitted signal to incident signal [44]. Over the years, this has advanced into the measurement of devices and systems that utilize wireless technologies.

[Weather radar systems]

Backscattering is essentially by microwaves that arrive at an object and are then diffusely reflected by either the shape/construction of the surface or bipolar molecular substances such as water when passing through the object. Examples in the field of weather radar system operation are Rayleigh scattering and Mie scattering, which are utilized to measure the backscattering of fine water droplets in the air. In Rayleigh scattering, when the wavelength is longer than the diameter of the water droplets in the air, backscattering is proportional to the object power multiplied by the object-specific reflection properties multiplied to the sixth power. In the case of Mie scattering, if the water droplet's diameter is close to the wavelength, diffraction in the direction of wave travel and optical refraction increases, and backscattering is diminished [39][45].

These systems are also not applicable to this experiment because they use higher-frequency bands with shorter wavelengths. Additionally, the required equipment is large in size, measures targets primarily from far distances and covers a vast area.

[UWB radar]

As reported, the measurement of water using microwaves is presently done only to measure small samples in a closed space or to measure wide-spread particles of water, like distant clouds. Accordingly, with these systems, it is difficult to measure backscattering at closer ranges, such as a few meters to several hundred meters, as is possible with the ultra-wide-band (UWB) radar.

UWB radar has the advantages of utilizing very low-power electromagnetic waves that are harmless to the human body and requiring very low average power to operate. Therefore, applied research in the field of medical welfare and the like is progressing. UWB radar can detect periodic movement, such as the limb motion, breathing, and heartbeat of humans. Other applications, such as underground sensing at short distances and collision avoidance of mobile devices such as automobiles, are being studied. One reported disadvantage is the difficulty involved in analyzing subtle changes in signal strength because, due to low power, it is susceptible to noise. Also, multiple sensors are necessary to expand the detection area [46][47][48].

[Synthetic Aperture Radar (SAR)]

Synthetic Aperture Radar (SAR) is a type of side looking radar system, the system can be installed on satellites and aircrafts which move in a high speed. By radiating the electric micro-wave in a special form and controlling the direction of the antenna precisely while it is moving, SAR system synthesize a big antenna in a SAR processor and it can generate high-resolution black and white images such as a map of the ground. Moreover, the images are able to be overlaid with the satellite image or a real

map etc., accurately, with SAR precisely measuring latitude and the longitude at the same time (Fig. 3-1).

There are numerous studies on soil moisture measurement. Most data collected for soil moisture are by using SAR or scatterometers mounted on satellites or airplanes equipped with different frequency bands. The measurement of soil moisture covers a wide geographical area; therefore, it is difficult to measure small areas, also it is hard to measure the same area every time its required by using SAR.

Measurement for vegetation covers the measurement of fields or farms such as corn, soybeans and wheat to monitor its conditions [49], also for forest observing [50]. Likewise, similar to soil moisture applications, most vegetation applications cover vast areas which make it difficult to monitor the status of the plants one by one to monitor its conditions.

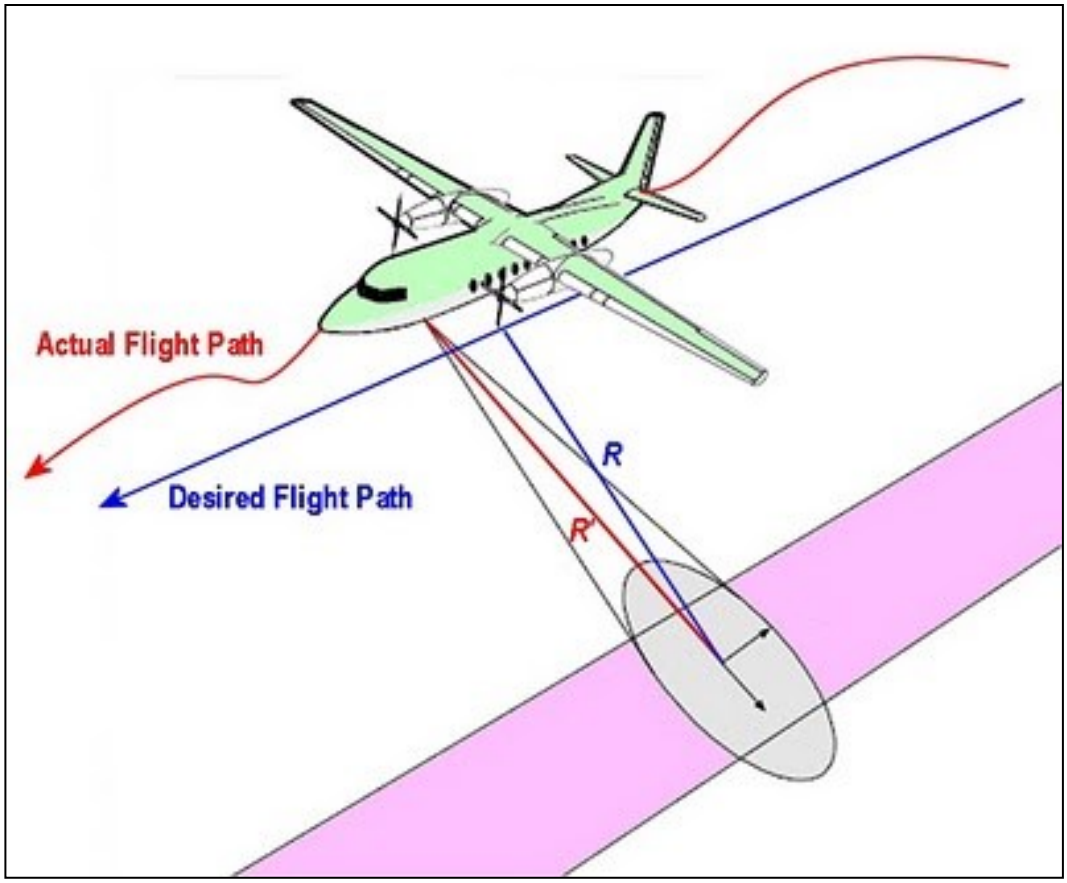

Figure 3-1 Airborne SAR system mounted on an aircraft while operation.

3-2 The Developed System for Backscattering Measurements

As explained in Chapter 1, the rapid evolution of microwave and electronics technologies has prompted the downsizing of devices and components, leading to the application of microwaves in fields in which the achievement of results capable of realizing practical use had, at one point, been difficult. One example is the field of remote sensing, which now utilizes advanced sensing technologies such as SAR. More compact equipment and systems also require less power to operate. For these reasons, it is believed that remote sensing technologies can now be utilized practically to create inexpensive and convenient tools for monitoring plant growth conditions in relatively isolated areas.

Making remote sensing equipment smaller and easier to use also creates the ability to resolve issues like measurement granularity and measurement distance, which were previously considered problematic.

[The proposed RCS measurement system]

This system will enable the measurement of trees individually from multiple directions and under a relatively wide range of natural growth situations. The device's main body is based on a SAR transceiver mounted on small aircraft. The compact size and lighter weight of the unit (i.e., the RCS measurement system) contribute to ease of handling, setup, and mobility. The system also requires significantly less power to operate than conventional SAR equipment.

As shown in Fig. 3-2, three RCS measurement systems were built for the experiments. All were constructed to enable stand-alone use and with customized

specifications that ensure highly useful features and convenience for the efficient remote sensing of vegetation in natural surroundings. Fig. 3-3 shows a sample illustration of the RCS measurement system configuration.

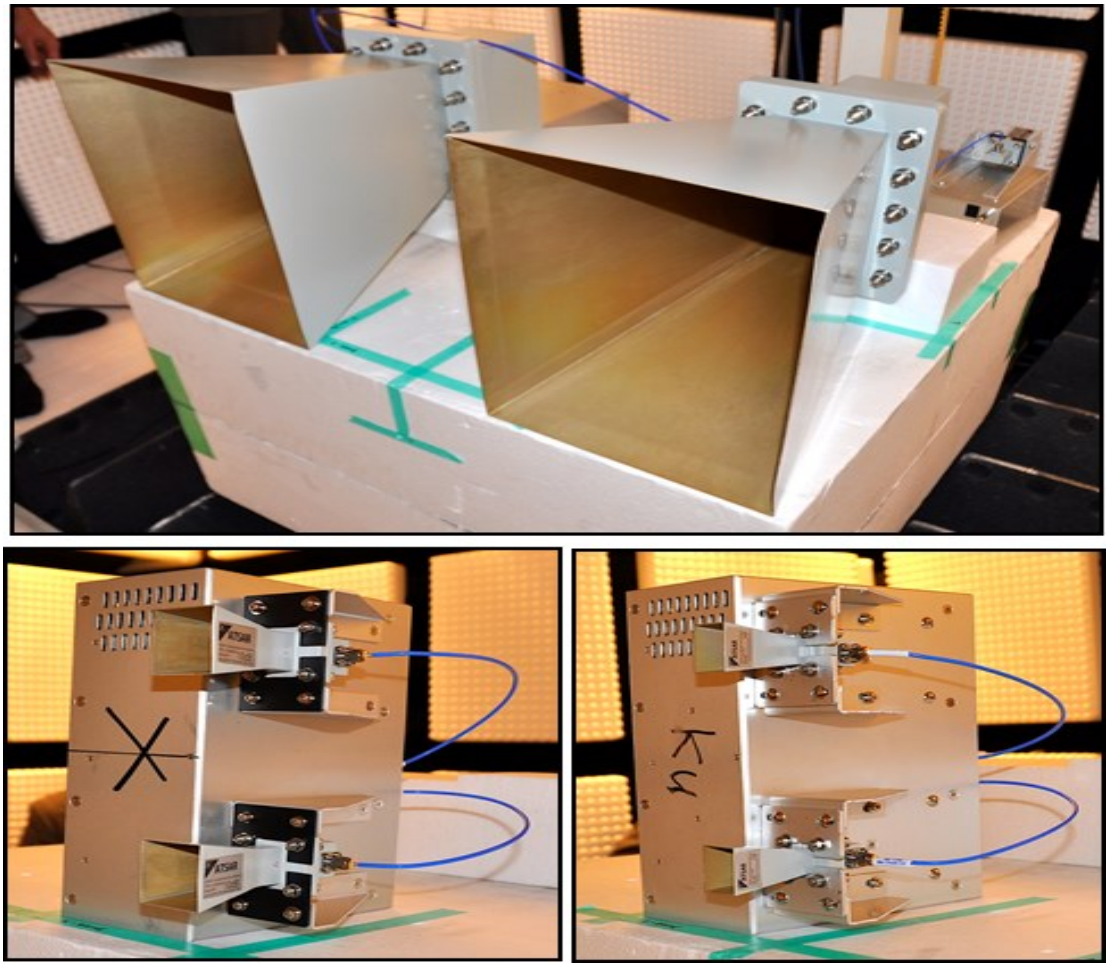

Figure 3-2 The RCS measurement system systems: L-band (top), X-band (bottom left) and Ku-band (bottom right).

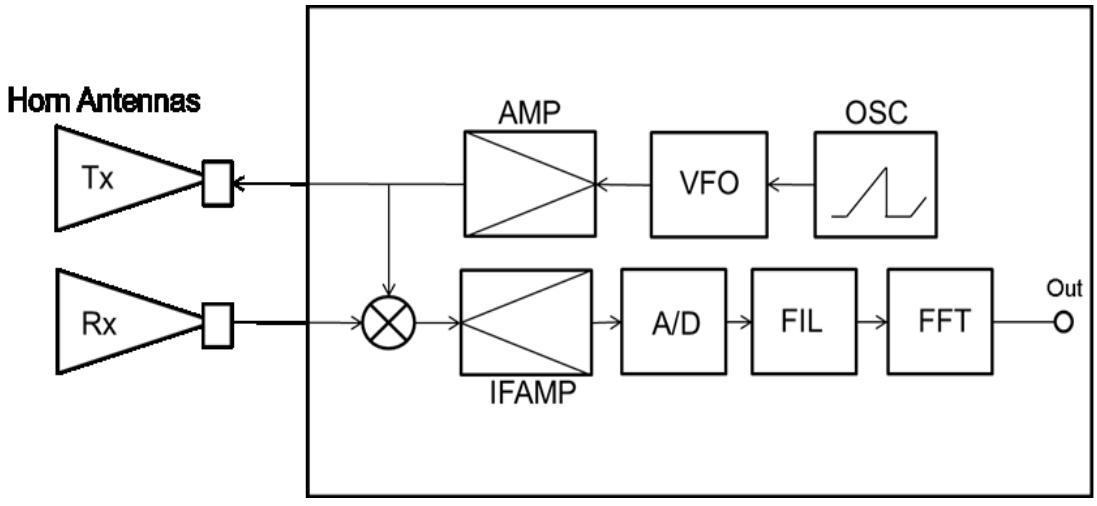

Figure 3-3 Configuration of the RCS measurement systems used.

One feature of the developed RCS measurement systems is that they enable time-domain measurement, which is the method of transforming the frequency domain into the time domain. This is convenient for calculating the distance of the object being measured, thereby allowing its position to be determined. Another feature is the use of frequency-modulated continuous wave (FMCW) transmission technology. This is useful because it enables the rapid and continuous measurement of objects in motion, which is beneficial because the objects in the experiments were placed on a rotator that turned 360º to subject the objects' entire surfaces to microwave irradiation. In practical terms, the rapid measurement of objects while in motion is beneficial because trees, while stationary, could sway due to the presence of wind, thereby possibly affecting measurement accuracy.

The RCS measurement system's other key features include low-power consumption/transmission, light weight, and ease of mobility. The fact that they can be operated utilizing a battery power source leads to a more affordable operating cost and enables the RCS measurement system's use in the field.

Table 3-1 provides a comparison of the RCS measurement system developed and a common VNA, thereby clarifying the reason for the utilization of the RCS measurement system. As shown here, the RCS measurement system operate at an amazingly fast speed of 1,250 measurements per second, which is ideal for measuring objects in motion and increases the feasibility of their practical use for measuring the water content of trees in the field.

Table 3-1 Comparison of RCS measurement system and common VNA features.

Features	RCS measurement system	VNA
Measurement Speed	800μs	0.1-1sec
Transmission technology	FMCW	STEP FM (Not suitable for radar)
Transmission power	100mW	10mW
Frequency bands	Ku-band = 17GHz X-band = 9GHz L-band = 1.2GHz	Open
Bandwidth	Ku-band = 300MHz X-band = 300MHz L-band = 85MHz	Based on antenna and measurement time

CHAPTER 4 - MEASUREMENT OF WATER CONTENT IN FOAM MATERIAL OBJECTS

4-1 Outline and Purpose of the Experiment

The goal of this study is to find the relationship between reflection intensity and water content by measuring microwave backscattering from a phenolic foam column with different water content in each microwave band.

The issues that must be considered in this experiment are as follows. The first is what can be learned from microwave backscattering measurements alone. One of the properties of microwaves is their ability to pass through nonconductive materials. In materials containing a bipolar molecular structure, such as water [51], the microwave generates a vibration that is converted to thermal energy. The amount of energy lost is proportional to the amount of water the material contains [52]. This suggests that a solid object's water content has a significant effect on the amount of energy that can penetrate the object. Additionally, water has reflective properties. When a microwave collides with the surface of water, part of the energy is reflected in a complicated manner, and scattering may occur depending on the conditions at that moment. Therefore, the total energy of a microwave radiated at an object is the sum of the transmitted energy, the amount of energy consumed internally as thermal energy, and the energy backscattered. This indicates that it is difficult to determine the absolute value of the water content in an object utilizing only the measurement of microwave backscattering intensity.

The next issue is the method of measuring and evaluating the intensity of microwave backscattering. Microwaves induce a fading effect because of complex reflections and repeated scattering due to the shape and size of the object to be radiated and to environmental factors in the surrounding area. Therefore, unambiguously determining the reflection intensity is a difficult task. Furthermore, because fading changes

considerably due to delicate differences, such as antenna position and object position, a complete reproduction of the measurement results is difficult as well.

In consideration of these points, in this study, phenolic foam columns (i.e., solid objects), each containing different volumes of water, were placed one at a time in an anechoic chamber, and microwave backscattering measurements were performed for each. Measurements were taken of the entire surface (the full circumference of the column), and the results compared considering each column's water content. To avoid influences other than water content, the objects were made of a cylindrical foam material that had a low relative dielectric constant, a high water absorption ratio per unit volume, and a simple and homogeneous internal structure. The microwave source was a low-power radar (FMCW) RCS measurement system. The bands used were L, X, and Ku, which were chosen assuming practical public use in the future. Finally, all the measurement results were evaluated using variance, average, and median.

4-2 Target Material

Cylindrical-shaped columns comprising multiple phenolic foam discs (Oasis Rainbow Foam, Item No. 37001) were measured. Each disc was 5 cm in height and 20 cm in diameter at the base. As shown in Fig. 4-1, by stacking the phenolic foam discs, a column of foam 75 cm in height and 20 cm in diameter at the base was formed. This material had a high water absorption capability, which was crucial for keeping the projected surface area constant while changing the volume of water content.

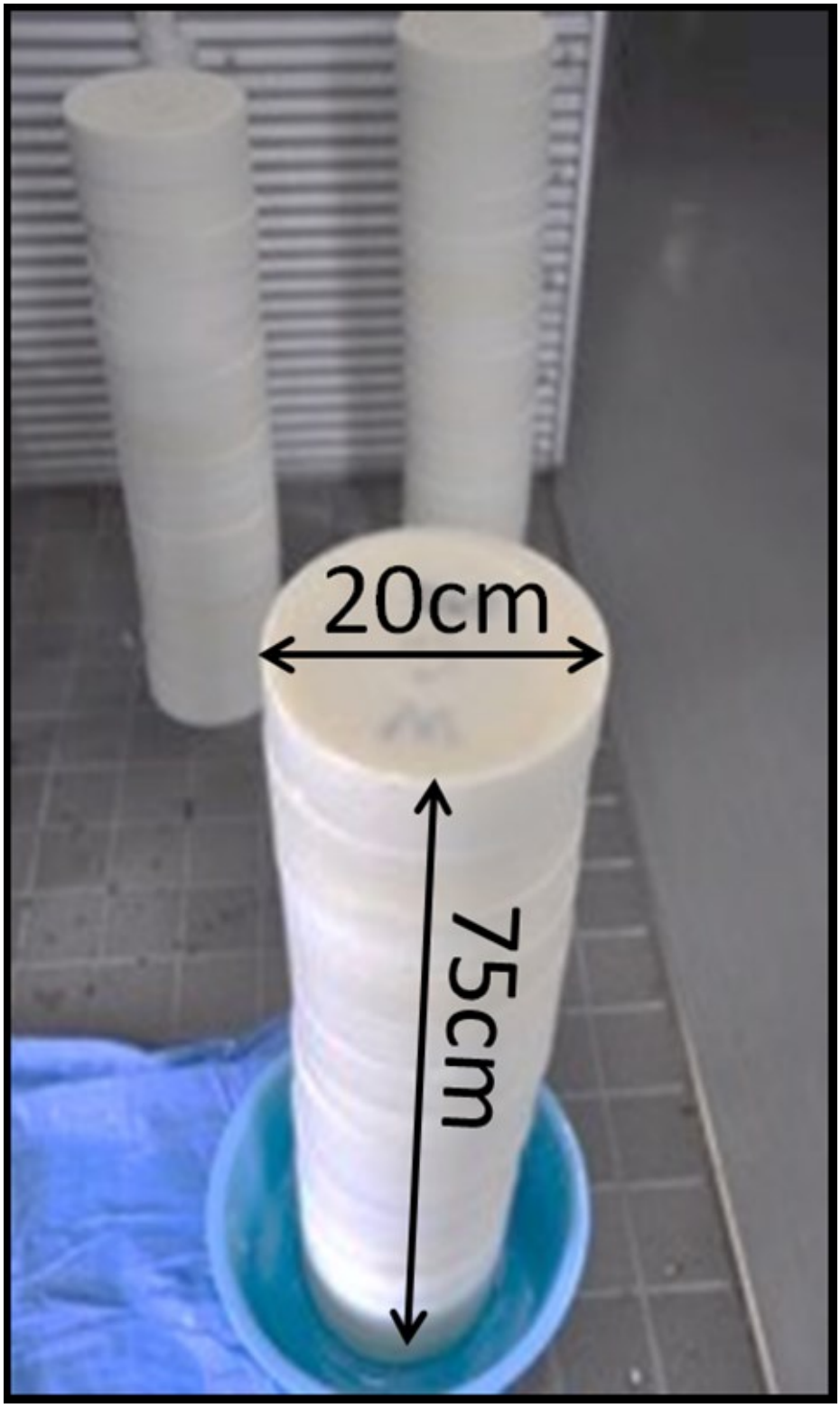

Figure 4-1 The phenolic foam columns used in this study.

4-2.1 Physical characteristics

Phenolic foam is made from a resin with a dielectric constant of 2.0 - 2.6. The foam resin used for this experiment had an expansion ratio of 1:45. The relative dielectric constant is lower than that of dry snow ice (relative dielectric constant = 3.3) and dry soil (relative dielectric constant = 2.5-3.0). Therefore, it is reasonable to conclude that the actual dielectric constant without moisture is considerably lower. Additionally, the surface is very smoothly formed, and individual cells are 0.3-0.5 mm or less, which is visually uniform.

4-2.2 Setup and experimental conditions for the columns

For this study, four water content conditions were prepared representing 50% (WTR50), and approximately 35% (WTR35), 25% (WTR25) and 0% (WTR0) saturation[1]. These percentages represent the volume ratio of water to the volume of the column. Table 4-1 shows the details and other typical materials.

Table 4-1. Volumetric ratio of phenolic foam column and water content.

Condition	Total weight (g)	Water weight (g)	Volume (cm^3)	Water weight to volume ratio
WTR0	650	0	23,562	0.00
WTR10	3,000	2,350	-	0.10
WTR25	6,000	5,350	-	0.23
WTR35	9,000	8,350	-	0.36
WTR50	12,000	11,350	-	0.49

[1] During the process of the experiment, a measurement failure occurred with the 10% (WTR10) water-content-level condition. It is assumed that this failure was due to the submergence of the sample into the water instead of the pouring of water into it. Submerging the sample caused water distribution in the phenolic foam to originate from the outside, seeping into the foam rather than being concentrated only inside under the surface. This adversely affected the reflection results for the WTR0 water-content-level approximation. Therefore, the results were not utilized for this experiment.

In related studies, water content is generally expressed as a weight to volume ratio. However, this experiment does not use weight to volume ratio. Rather, percentages are used. This is because the water does not disperse evenly in the column, as described below. Here, if the water content is indicated by the volume ratio, a misunderstanding may result.

One of the obstacles faced in this experiment was controlling the distribution of water in the column, which may have affected backscattering measurements and analysis results. To investigate the variation in water distribution in a phenolic foam column, a test was conducted using colored water. Four different water content conditions (WTR50, approximately WTR35 and WTR25, and WTR0) were created by slowly adding colored water to the pieces of foam. After production of the four water content conditions, the foam pieces were cut in half to enable observation of the internal water distribution. Fig. 4-2 shows the results of this test, indicating that the water distribution is different for each water content volume.

During preparation of the columns for measurement of the water content, the even distribution of water throughout the objects was difficult to achieve. Therefore, because the deviation of the column's moisture content causes fading, it has a significant effect on the variation in microwave backscattering intensity. To avoid this influence, the columns were rotated on a turntable to enable measurement results for the entire column surface (circumference).

4-3 Experimental Design and Process

Foam columns containing different volumes of water were placed in an anechoic chamber and were irradiated with microwaves one at a time. The backscattering

intensities were recorded to detect each object's water content. A detailed description is provided hereafter.

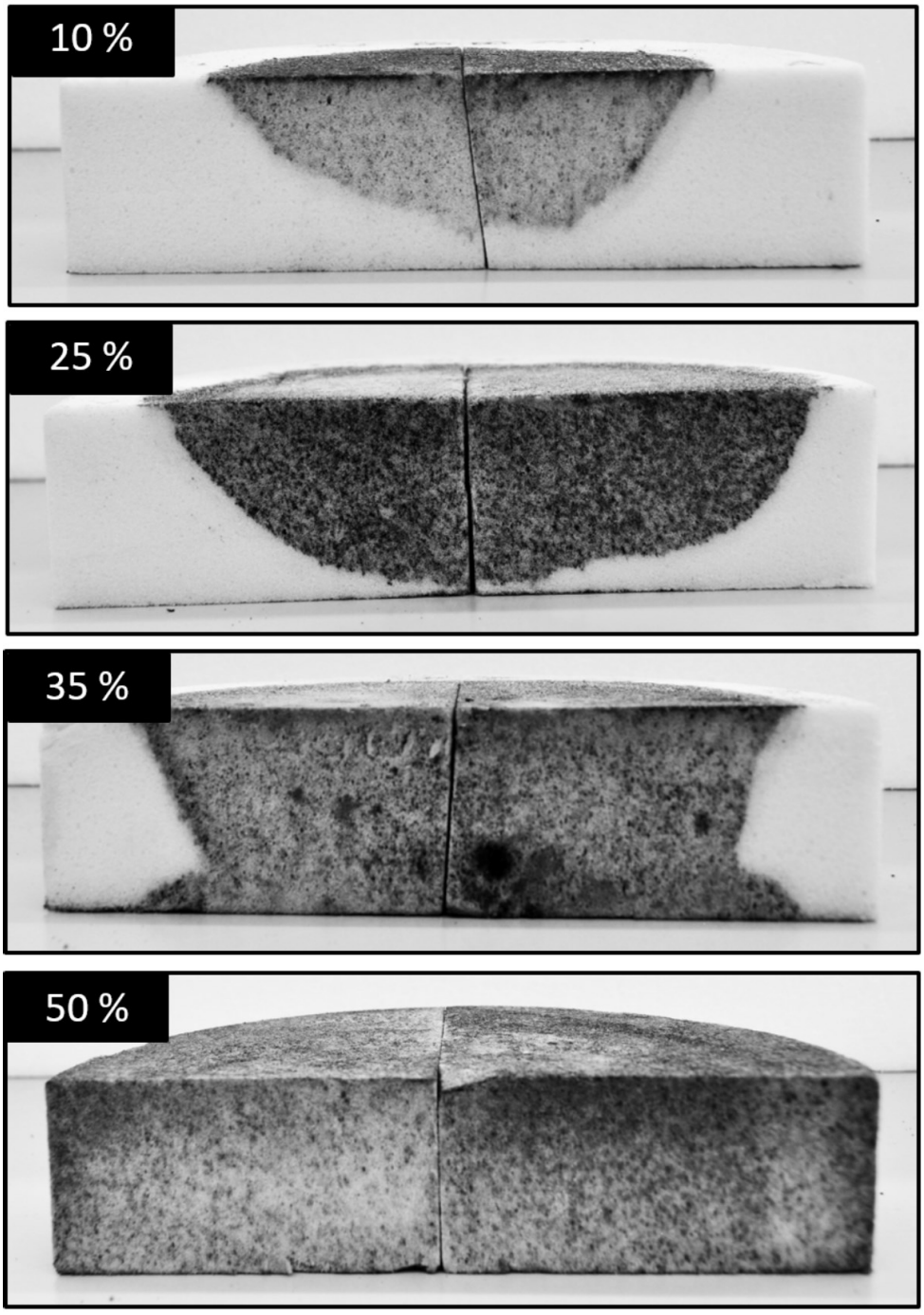

Figure 4-2 Distribution of water absorbed by each piece of phenolic foam for each level of water content.

4-3.1 Apparatus

The apparatuses required for the experiment included an anechoic chamber in which the measurements were carried out. Three RCS measurement systems were each set to a different frequency band and equipped with two horn antennas, a rotator (i.e., a motorized table capable of turning the object 360°), and a computer system for controlling the RCS measurement systems, storing the measurement data and analyzing the experiment's results. Fig. 4-3 illustrates the overall experimental setup.

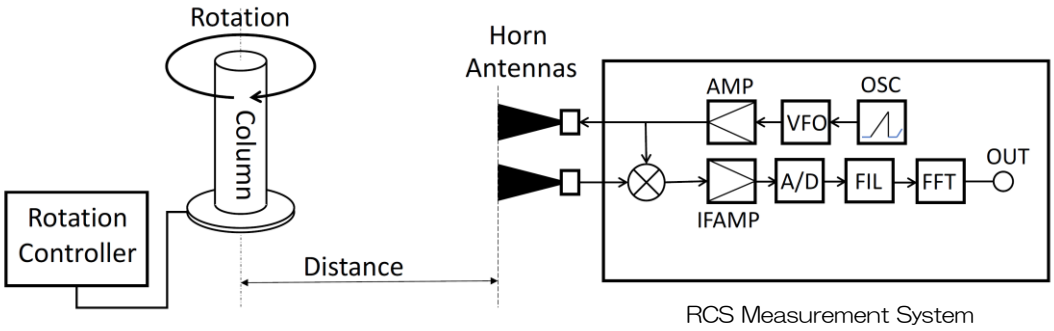

Figure 4-3 Schematic diagram of the experiment configuration; the RCS measurement system, rotating table, phenolic foam column and rotation controller were placed in an anechoic chamber, with the rotating table holding the column positioned 2.9m from the system.

[Anechoic chamber]

To ensure that only backscattering from a specific object was measured, the researchers had to minimize the reflection of microwaves from objects other than the one being targeted. Furthermore, in addition to eliminating possible interference, because the experiments were conducted in Japan, compliance with the Japan Radio Law was necessary. This was achieved by carrying out all measurements in an anechoic chamber, thereby creating a fully controlled environment that allowed measurements to focus on the relationship between the microwaves and water content

volume of each object. The dimensions of the anechoic chamber were 5 meters in length, 3 meters in width and 1.9 meters in height (Fig. 4-4).

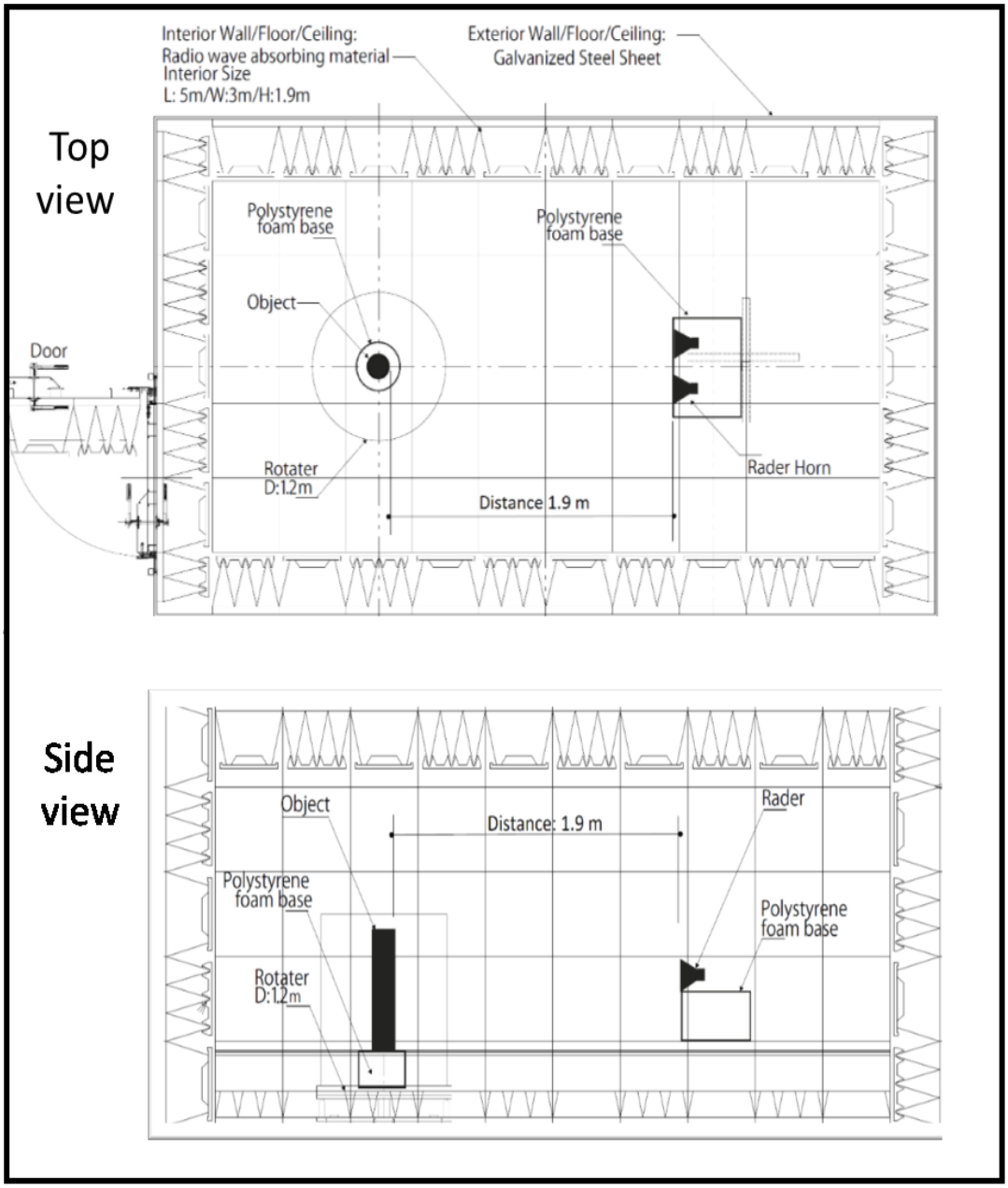

Figure 4-4 The anechoic chamber.

[RCS measurement systems and horn antennas]

Table 4-2 presents the RCS measurement systems' specifications. The three frequency bands chosen were the L-, X- and Ku-bands, those most commonly used for remote sensing.

Table 4-2 RCS measurement system specifications.

Band	L	X	Ku
Modulation	FMCW	FMCW	FMCW
PRF [μs]	800	800	800
Frequency [GHz]	1.2	9	17
Bandwidth [MHz]	85	300	300

The antennas for each frequency band had different specifications as well, as presented in Table 4-3.

Table 4-3 Horn antenna specifications.

Band	L	X	Ku
Size [mm] W×H	384×284	42×35	32×23
Antenna gain [dB]	14.52	11.29	14.62
3dB Beam width	55-degree Typ.	55-degree Typ.	55-degree Typ.

[Rotator]

The objects to be measured were placed on a rotator that completed one full rotation every 60 seconds, enabling the measurement of the entire circumference of the object sitting on it. The rotator diameter was 1.2 meters, and it was positioned directly in front of the middle of the antennas at a distance of 2.9 meters. It was operated by a control system located outside the anechoic chamber.

[System control]

The computer system used to control the RCS measurement systems and collect the measurement data during the experiments was a laptop employing the Microsoft Windows operating system and using custom-made software created by the company that developed the RCS measurement systems.

4-3.2 Measurement method utilizing the RCS measurement system

The first determination to make was which microwave frequencies to utilize for the experiments. Microwaves have different penetration depths depending on the wavelength irradiated [53]. Longer wavelengths penetrate deeper, and the possibility of detecting internal changes inside the object is higher. For this reason, the L-band microwave frequency was chosen. Additionally, shorter wavelengths, like X-band or Ku-band microwaves, are suitable for capturing changes in shape at the surface. Each of these wavelengths is known to have intrinsic characteristics, and these three frequencies are the most commonly used bands in the remote sensing field. Therefore, the decision was made to utilize the L-, X- and Ku-bands.

The issue of fading is also important, as its influence always appears when microwaves are used to take measurements. Multipath fading caused by the object being measured is the result of complicated microwave reflections and scattering due to the object's surface shape and/or internal composition. Accordingly, analysis of the fading pattern enables the observation of changes in the object. Therefore, the multipath fading caused by the objects' shape and internal composition was measured by analyzing the measurement data of the entire circumference. To achieve this, the RCS measurement systems were set to continuously measure backscattering, doing so at a very high speed.

The RCS measurement systems developed can conduct high-speed measurements at a close range (i.e., one meter to several kilometers). Additionally, the minimum resolution range was 170 cm for the L-band, and 50 cm for the X-band and Ku-band.

As previously mentioned, each band has unique characteristics and different penetration levels. Each RCS measurement system was connected to horn antennas designed to be polarized vertically VV and horizontally HH when rotated 90º, except for the L-band, for which only VV was used due to the chamber's limited size and the antennas' large size.

4-3.3 Experiment process

The three RCS measurement systems, each equipped with a different frequency band (i.e., L, X, and Ku), were placed in the anechoic chamber one at a time and used to irradiate the objects. Each object's microwave backscattering intensities were measured; the backscattering intensities were captured and recorded, and later analyzed to determine differences in the characteristics of the objects' surface and internal structure. Before the measurements were taken, the three RCS measurement systems were calibrated using a trihedral corner reflector with a surface area of 0.1 meters.

Each object was set on the rotator, one at a time, and separately measured using each frequency band and both VV and HH polarizations, except for L-band HH polarization.[2] During measurements, the RCS measurement system was connected to a laptop computer located outside the anechoic chamber. The computer controlled the rotator speed and RCS measurement system operation, and was equipped with

[2] Due to space limitations for antenna placement in the anechoic chamber, the large size of the L-band antennas did not enable their use in an ideal position for HH polarization. Placing them close to each other would have caused antenna-to-antenna coupling and interfered with the measurement results. Thus, HH polarization for the L-band was not conducted.

custom-made software for recording the raw data measured. The raw data was later processed to determine the received power S_R, which was used to calculate each object's RCS.

During measurement, the rotator turned a full 360º for a period of one minute. This enabled the consideration of fading's influence by measuring microwave backscattering over the entire surface of the object and conducting a statistical analysis of the results.

To determine the position of the object during each measurement, the RCS measurement systems measured backscattering applying the FMCW time domain method. The bandwidths were set at 85 MHz for the L-band and 300 MHz each for the X-band and Ku-band. Therefore, the range pixel size was 1.7 meters for the L-band, and 0.5 meters each for the X-band and Ku-band.

The RCS measurement systems were set to take one measurement per 800 microseconds (μs). Because measurements were continuous, 1,250 data points per second were obtained. This enabled investigation of the effects of measurement and noise, and measurement of the data's variance and median. Furthermore, this level of data collection helped ensure the accuracy of measurements.

Throughout the experiment, the objective was to obtain the RCS values for each object and to determine the objects' conditions based on those values. The calibration values obtained for the three RCS measurement systems before starting the experiments were used as reference data when calculating the RCS values.

4-3.4 Measurement procedure

Each measurement was divided into three parts. In the first part, the three RCS measurement systems were calibrated using a trihedral corner reflector with an edge dimension of 0.1 m. Calibration for polarization was conducted as well. The results of

the calibration were used to calculate the column's RCS and applied as a reference to estimate the column's position.

The second part tested the phenolic foam column for four water content conditions. The first measurement was conducted using the column containing the maximum amount of water it could absorb (WTR50). Columns with water volumes of approximately WTR35 and WTR25, respectively, were measured next. The fourth and final measurement was a column with no water (WTR0). For each condition, the column was rotated as explained above and separately tested for both polarizations, irradiating with the three frequency bands, one at a time. To provide a baseline for comparison with the other conditions, backscattering was measured for 10 seconds without using a column (referred to as "NO").

Each RCS measurement system was set to execute one measurement per 800 μs; therefore, during a 60 seconds, approximately 75,000 data points were recorded per range pixel. The RCS measurement systems were connected to a computer equipped with custom-made software that collected the raw data during the measurements. After the experiment, the raw data collected from the RCS measurement systems was processed to determine the energy reflected (S_R) by the column. This was later used to calculate each column's RCS value.

The last part involved ensuring that the phenolic foam used was susceptible to penetration by microwaves. An experiment using a spectrum analyzer was conducted to test the penetration level for the different water content levels. The column was placed between the RCS measurement system and the spectrum analyzer receiver antenna, and the microwaves that penetrated the column were measured using the spectrum analyzer. As shown in Fig. 4-5, the receiving antenna of the spectrum

analyzer was held by hand and positioned near the column (3-5 cm) on the opposite side of the column facing the RCS measurement system to measure the attenuated power. A measurement was also taken without placing a column between the RCS measurement system and the antenna.

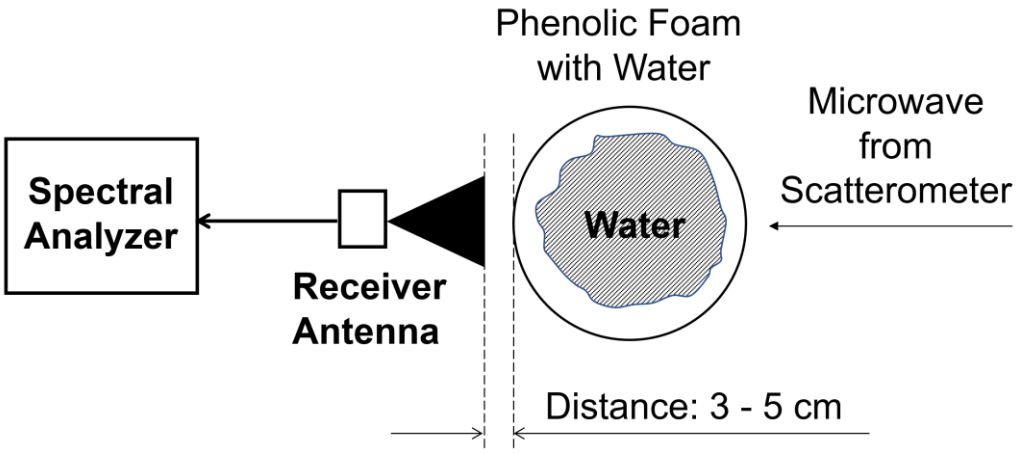

Figure 4-5 The data collection process for the phenolic foam column microwave penetration test.

4-4 Results

The purpose of this experiment was to investigate the characteristics of microwave backscattering and determine whether direct microwave backscattering can confirm different water content volumes in objects. Due to the similarity of the results for the VV and HH polarizations, only VV polarization graphs are presented. It was found that, using the method the author applied, measuring and analyzing microwave backscattering is possible to determine water content volume in different objects. The results of the experiment are provided hereafter.

4-4.1 Validity of the data

First, to confirm the validity of the data, the RCS measurement systems were calibrated and the baseline data measured using a corner reflector as the target object. In Fig. 4-6 (A), the measurement results for the microwaves of the three frequency bands reflected off the corner reflector are shown as variation rates. The fluctuations in the microwave intensities of each band reflected off the corner reflector were minimal; all were within ±0.4%. In addition, the RCS measurement systems used in this experiment recorded data measurements as a complex number. This enables phase analysis of the data. The phase is determined by the distance from the antenna to the column. Therefore, the amount of phase shift can be converted into the change in the distance between the antenna and the column. That is, a check of the phase shift fluctuation can confirm whether the measurements were taken correctly. In Fig. 4-6 (B), the phase shift variation rate is shown in the results measured for the corner reflector. Here, it is found that the phase shift variation rate is stable at ± 3° or less. All the data measured was checked by phase shift based on the above, and the stability and accuracy of measurements were confirmed. Additionally, measurement results for which the phase shift fluctuation rate was extremely large were deemed to be failed measurements and were excluded from the evaluation.

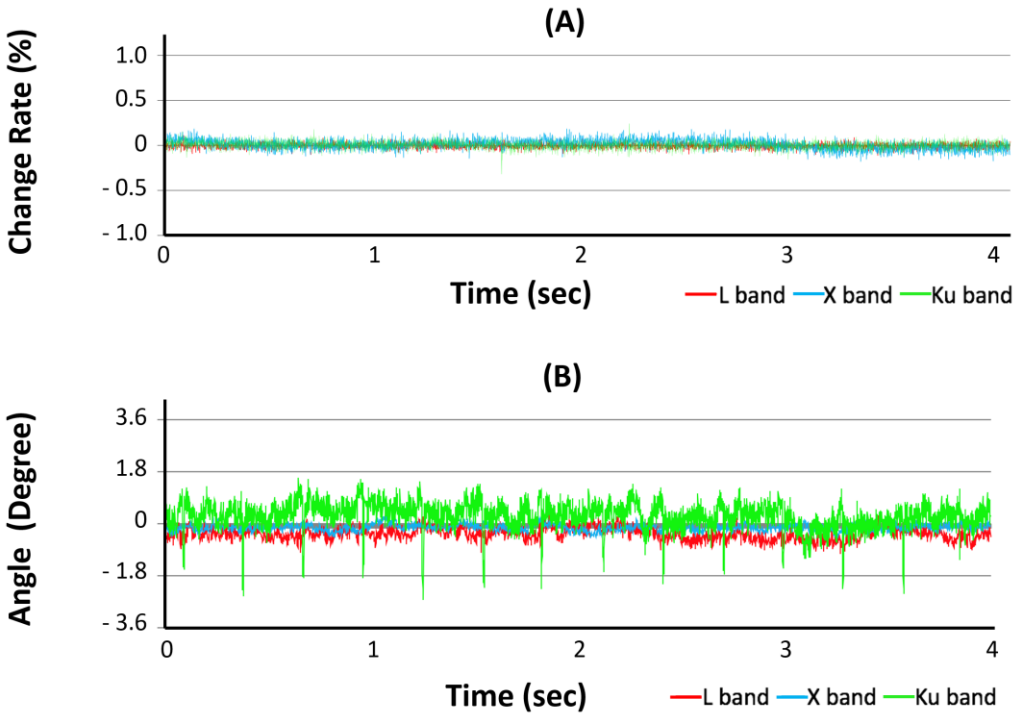

Figure 4-6 Variation in the ratio of (A) backscattering intensity from the corner reflector and (B) phase shift as the result of VV polarization.

4-4.2 Microwave penetration to the target column

Figure 4-7 shows the microwave penetration power values measured for four columns with varying water content levels (i.e., WTR0, WTR25, WTR35, and WTR50) and without a column (NO). The receiving power of WTR0 and NO are almost the same value. This means the column's attenuation can be negligible. In more detail, the microwave penetration power decreases as the column's water content increases between WTR0 and WTR35 in all bands. However, such a reduction is not seen between WTR35 and WTR50.

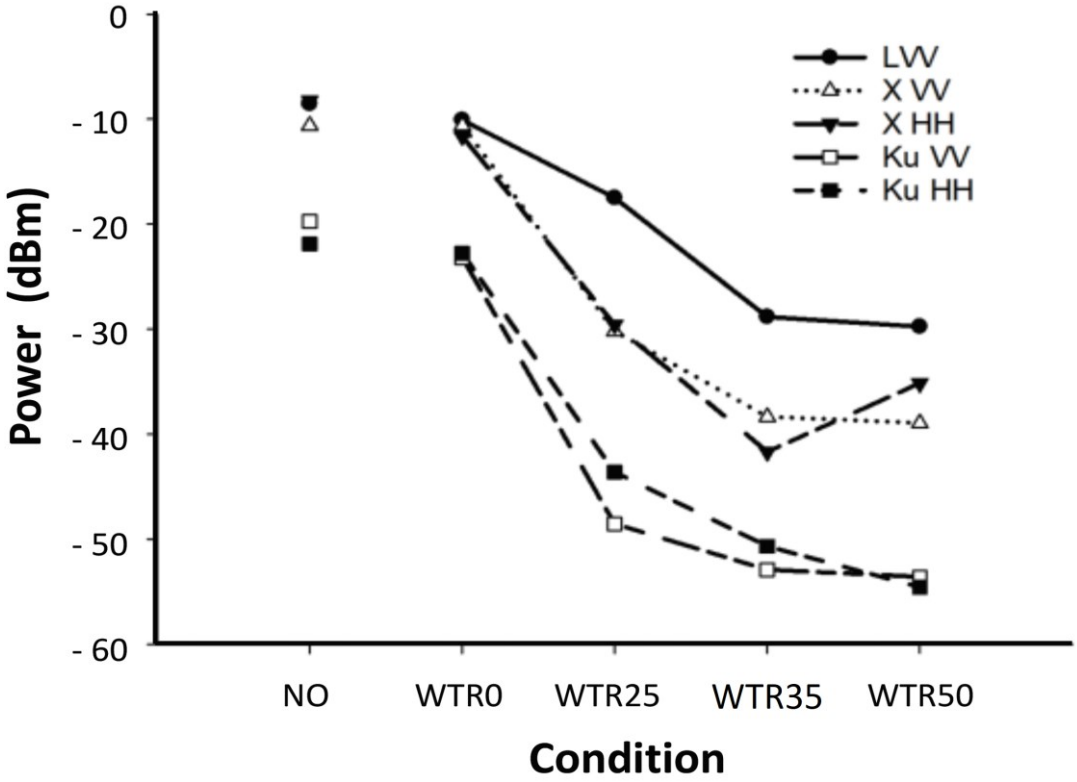

Figure 4-7 The penetration results of the phenolic foam columns.

The following reasons are conceivable. Figure 4-2 is a cross-sectional image of the column showing a change in water content area due to an increase in water penetration. As shown here, from WTR0 to WTR35, the distribution of water inside the column gradually expands from the center towards the outer surface. Additionally, as shown in Fig. 4-5, the spectrum analyzer receiving antenna is positioned very close to the column. For WTR0 to WTR35, as the distribution of water content expands from the center portion of the column, the shielding area of the opening in the receiving antenna expands but is almost completely shielded at approximately WTR35. Therefore, attenuation of the microwave penetration level decreases as water content increases from WTR0 to WTR35. The results of the microwave penetration test indicate that, for L-, X- and Ku-bands, it is possible to distinguish the water

content inside the column between WTR0, WTR25 and WTR35 using the penetration level. However, it is not possible to distinguish between WTR35 and WTR50.

4-4.3 Measurement results and analysis

Figure 4-8 shows examples of measurement results (WTR35 in L-VV, X-VV, and Ku-VV). Each column was placed on the turntable individually and rotated at a constant angular velocity. Then, the data during the 360° rotation was measured. In this figure, the vertical axis shows the RCS calculated from the reflected power, while the horizontal axis indicates the column's rotation angle.

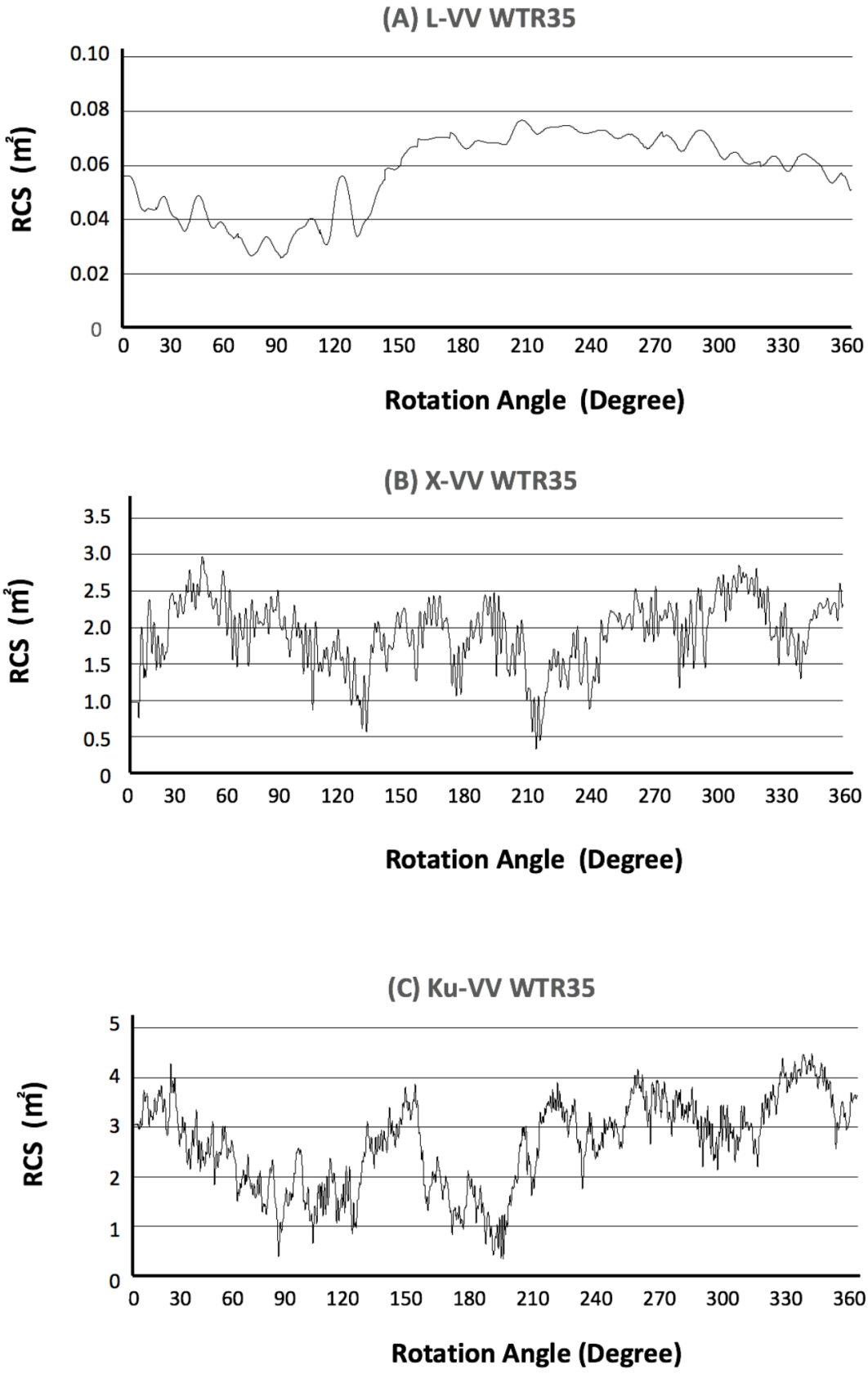

Figure 4-8 The L-VV, X-VV and Ku-VV measurement results for one full rotation of columns with water content of WTR35.

These results show significant fluctuation during column rotation. It is believed that this is because many microwave reflection points are scattered inside the column. That is, the microwave radiated from the transmitting antenna is reflected by the reflection points scattered inside the column, and amplitude fluctuation occurred because of the phase difference of the receiving signal during the column's rotation. Additionally, the phase shift due to the change in path length is proportional to the microwave's frequency. The fluctuation of the RCS caused by rotating the column (Fig. 4-8) shows fast fluctuation at a high frequency (Ku-VV) and slow fluctuation at a low frequency (L-VV). Therefore, this experiment's measurement results represent the microwave reflections off the water inside the column, which was considered appropriate for conducting an analysis and evaluation using a statistical method. Therefore, for subsequent measurement results, RCS is expressed as a statistical value.

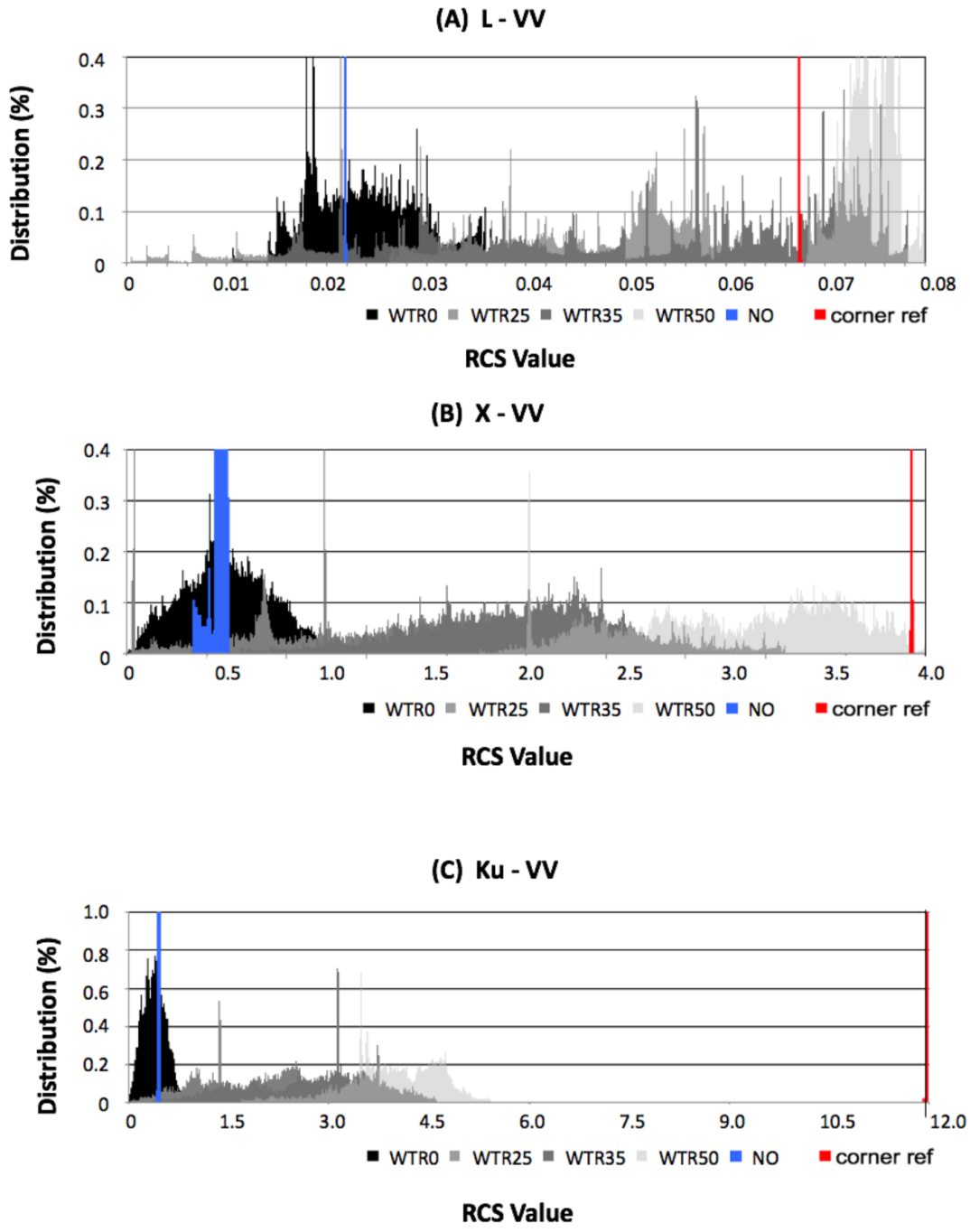

Figure 4-9 The RCS distribution charts of backscattering measurement results for WTR0, WTR25, WTR35 and WTR50, NO, and CR.

Figure 4-9 shows the results of microwave backscattering measurements using a histogram. The four measurement results of the column, NO, and corner reflector (CR) are shown for each of the three frequency bands. Each graph's horizontal axis represents the value of RCS with a linear scale. In the case of CR and NO, because the measurement results are irrelevant to the turntable's rotation, it is almost constant

for all bands. However, only in the case of X-VV are there slight fluctuations in the NO results. It seems that this fluctuation is caused by a reflected wave from the rotating table itself. In addition, although some fluctuations are seen in WTR0 for all three bands, this indicates that phase attenuation due to the column is hardly observed, though phase variation due to the propagation path is observed. However, because the measurement results for NO are located near the median value of the measurement results for WTR0, it can be said that the average measurement results for WTR0 are no different from the results for NO.

Based on the results of this and Section 4-4.2, it is believed that the column used in this experiment has a sufficiently high permeability to radio waves. Therefore, it can be said that the measurement results for WTR25, WTR35, and WTR50 are almost entirely the backscattering intensity from the column's water content.

CHAPTER 5 – MEASUREMENT OF WATER CONTENT IN PALM TREE TRUNKS

5-1 Outline and Purpose of the Experiment

As the follow-on to the positive results of previous experiment, the RCS measurement systems developed were utilized to measure the intensities of microwaves backscattered from palm tree trunks irradiated from all sides to determine whether the methodology is applicable to the practical monitoring of actual trees [57].

Figure 5-1 Sago palm tree.

The tree species chosen as the object of measurement was the sago palm (i.e., *Cycas revolute*), a tree found in Japan that is the most similar in structure to the date palm trees of the Middle East (Fig. 5-1). For purposes of this experiment, to simulate the conditions of a red palm weevil infestation of a date palm tree, the trunks of healthy sago palm trees were harvested, truncated and subjected to periodic measurement of microwave backscattering intensity for three months. The measurements recorded throughout the experimental period were then analyzed to determine whether changes in the tree trunks were detectable.

5-2 Target Material

The objects measured in this experiment were palm tree trunks, as most of the water that palm trees contain is in their trunks [58]. To prepare a trunk-only form, the stems, leaves, and roots were removed. This also allowed for more accurate detection and monitoring of internal change. Additionally, to promote the drying process, an incision the length of the tree trunk was made, as were two holes—one each at the center of the top and bottom of the tree trunk.

Because trees have unique characteristics (e.g., size, weight, and water content), 10 palm tree trunks were prepared as the sample through which to compare changes in surface and internal conditions over time (Fig. 5-2). Date palm trees do not grow in Japan; thus, the sago palm tree (i.e., *Cycas revoluta*) was used as a substitute. To measure and monitor the entire surface of each object, the tree trunks were placed one at a time on a slow-turning rotator, and each trunk was turned 360º during irradiation, enabling the measurement of changes in the trunks from all angles.

Figure 5-2 The 10 palm tree trunks used.

5-3 Experimental Design and Process

5-3.1 Apparatuses

This experiment utilized the same equipment utilized for previous experiment in chapter 4. These devices were equipped with the features and specifications required to conduct remote sensing backscattering measurements in a natural setting.

All measurements were conducted in the same anechoic chamber. Time-domain measurement was incorporated, enabling the extraction of only the reflection intensity from a specific distance. Fading was also considered. Other experimental parameters were equivalent to those specified for Experiment 1.

5-3.2 Palm tree trunk preparation and care during the experiment

Artificially introducing sudden changes in the state of a living tree, such as damage caused by pest infestation, is a difficult task. Therefore, to simulate this state, the palm trees were truncated, thereby cutting off the ability of water to enter the tree via the root system. In addition, to promote drying, two holes were bored the length of the tree trunk, from the center of the top to the center of the bottom (Fig. 5-3). The average characteristics of the individual trees were also compared.

Figure 5-3 Tree trunks after preparation.

To measure moisture loss, the weight of each tree trunk was recorded every few days. Weight measurements were conducted on the following dates: 10 April, 28 April, 2 June and 23 June 2015. Table 5-1 shows the palm tree trunk weights for each day.

Table 5-1 Palm tree trunk weights on dates measured.

Tree weight table (kg)				
Tree No. / Date	4/10	4/28	6/2	6/23
1	29.51	28.09	22.35	19.23
2	24.24	22.95	17.99	15.12
3	24.92	23.68	18.64	15.98
4	20.33	19.3	14.91	11.76
5	21.38	20.17	17.29	15.78
6	13.79	13.25	10.39	9.13
7	19.59	18.74	15.62	13.89
8	17.82	16.87	13.70	11.75
9	18.08	17.4	15.12	14.07
10	11.05	10.49	8.26	7.18

At the time of tree trunk preparation, each trunk was measured for diameter and thickness. The projected area was calculated, as shown in Table 5-2.

Table 5-2 Tree trunk measurements.

Tree No.	Diameter	Thickness	Projected Area (m)
1	0.230	0.720	0.166
2	0.195	0.755	0.147
3	0.220	0.655	0.144
4	0.200	0.675	0.135
5	0.205	0.635	0.130
6	0.200	0.590	0.118
7	0.180	0.645	0.116
8	0.195	0.580	0.113
9	0.185	0.610	0.113
10	0.180	0.485	0.087

5-3.3 Measurement process

As in the previous experiment, the RCS measurement systems were first calibrated using a trihedral corner reflector with a surface area of 0.1 m. Next, the palm tree trunks were placed on the rotator, one at a time, and measured separately using each frequency band and both polarizations (Figs. 5-4, 5-5 and 5-6). The RCS measurement systems were connected to the same computer utilized for the first experiment. The same software was used to record and collect the raw data measured.

The raw data was then processed to determine the received power S_R, which was used to calculate the RCS values for each palm tree trunk.

Figure 5-4 The palm tree trunk L-band measurement.

Figure 5-5 The palm tree trunk X-band measurement.

Figure 5-6 The palm tree trunk Ku-band measurement.

5-3.4 Measurement parameters and equations used

The objective of this experiment was to calculate the RCS values of palm tree trunks at different stages of tree health (simulated by trunk moisture content), thereby determining the possibility of non-invasively determining palm tree health in a natural environment.

The RCS measurement systems were set to take one measurement every 800 microseconds (μs). Bandwidths were set to 300 MHz for the Ku-band and X-band, and 85 MHz for the L-band. Additionally, the data recorded underwent dedicated processing until the plotting of the final results.

5-3.5 Data processing

First, the data recorded (i.e., backscattering intensities from objects) was transformed from time scale to distance scale using Fast Fourier Transform (FFT). Next, the object position was determined based on the distance between the antenna and the object (i.e., measured manually in meters in the chamber before the experiment). The object position in the data was displayed in pixels, with the pixel range being 1.7 meters for the L-band and 0.5 meters each for the Ku-band and X-band.

Next, the microwave backscattering intensities were calculated. The data compiled comprised very complex numbers, equaling the summation of the microwaves reflected from every point on the object. The sum of the backscattering intensity from the object at specific angles was determined by calculating the amplitude's absolute value. The data measured was then converted into RCS values using the reference data obtained from the corner reflector during RCS measurement system calibration. Finally, the RCS values calculated were plotted to display the distribution of values,

and the changes in the conditions of each palm tree trunk on the various measurement dates were compared.

If only the average of the RCS values (data points) is calculated based on measurements during rotation, accounting for and showing the meaningful differences in the reflected RCS values may not be possible. Therefore, to clearly show the data's validity, the RCS value distribution of all measurements (i.e., not the average RCS value) was plotted.

5-4 Results

Due to the similarity of the results for the VV and HH polarizations, only VV polarization graphs are presented. Additionally, it should be noted that failed measurement attempts were experienced for the first three palm tree trunks (i.e., Nos. 1, 2 and 3) using the Ku-band RCS measurement system on day 53 and for all the palm tree trunks using the Ku-band on day 74. In addition to histograms, RCS maximum (max), mean (mean) and minimum (min) values are used to show the distribution of RCS values.

Fig. 5-7 shows the results of plotting the number of days on the horizontal axis and the change in mass on the vertical axis. The results indicate that although some differences exist in each data set, mass loss was almost linear for all tree trunks. Although a difference exists in reduction rate, considering the difference in volume and mass, the loss was almost the same for each trunk.

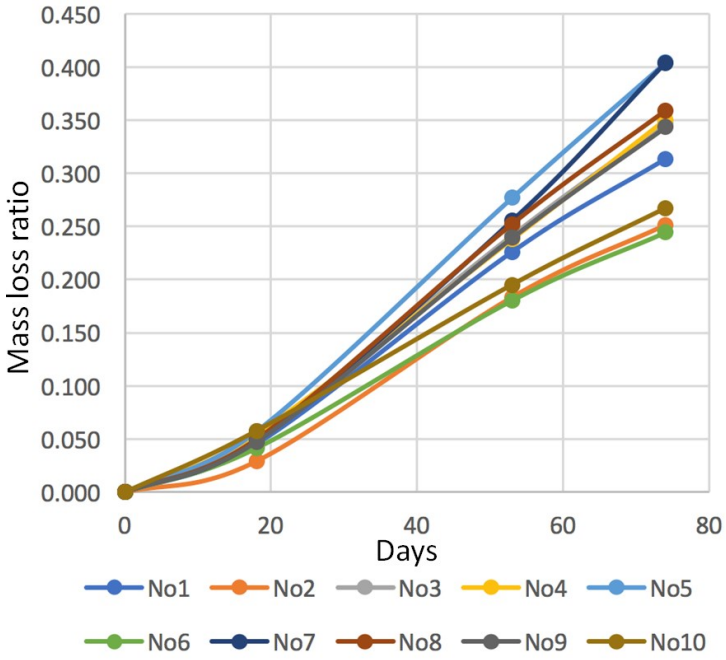

Figure 5-7 Mass loss from the palm trees during the experiment period.

The values obtained reveal a smaller mass, which is believed to be related to various factors, including loss of moisture. The graph shown here reveals that the mass of each palm tree trunk decreased almost linearly during the three months after the trees were harvested.

5-4.1 Evaluation considerations

During evaluation of the measurements, the following issues were considered:

1) All the measurement data was converted into RCS values and the results displayed in a linear-scale graph. Because comparing the results of each measurement is a vital component of this experiment, all measurement results were converted into RCS values. Generally, microwave measurements are displayed logarithmically; however, this study displays the data utilizing the linear-scale order to compare shapes using a histogram.

2) To obtain the most accurate measurement results, evaluations used the maximum value (max), minimum value (min) and mean value (mean). In addition, a histogram

of the results measured using the entire surface of the tree trunk was created. During the taking of microwave measurements, depending on the positional relationship between the object and the measuring device/antenna, finding a fluctuation in the measurement results due to fading is possible. A method to suppress fading's influence was applied through the collection of a significant amount of data by rotating each object 360º and analyzing the results utilizing dispersion.

3) Measurements were taken four times over 74 days period. The first set of measurements was taken on the first day, the second set on the day 18, the third set on the day 53, and the fourth and final set on the day 74.

For each set of measurements, the same procedure was followed. To simulate as natural a setting as possible at the time of measurement, the tree trunks were stored in a dark, well-ventilated location with a stable temperature and humidity. Because the expectation was that a period of time between measurements would be required to allow the moisture content to fall based on natural evaporation, measurements were conducted at intervals of two to five weeks.

5-4.2 Exclusion of inconclusive data

The graphs of each band plotting the change in maximum, mean and minimum RCS values for the ten tree trunks are shown in Figs. 5-8, 5-9 and 5-10. The measurement dates are plotted on the horizontal axis. Based on the results plotted in the graph, the L-band measurements show a definite tendency among the results. For tree trunks No. 1 and No. 6, the RCS values are slightly lower than the others. A possible reason for this is that a tree trunk of shorter length and/or thinner physical size is generally believed to result in a smaller projected area. Tree trunk No. 1 was visibly thinner and shorter than the other tree trunks; therefore, the fact that the measured RCS values are lower is understandable. However, regarding tree trunk No. 6, although the

measured RCS values were low on average, there is little difference in size compared to the other trees. Accordingly, the reason for the lower values is unknown. Because the measurement values for tree trunks No. 1 and No. 6 showed a different tendency in the graph plotting RCS values and elapsed days, they are excluded from further discussion.

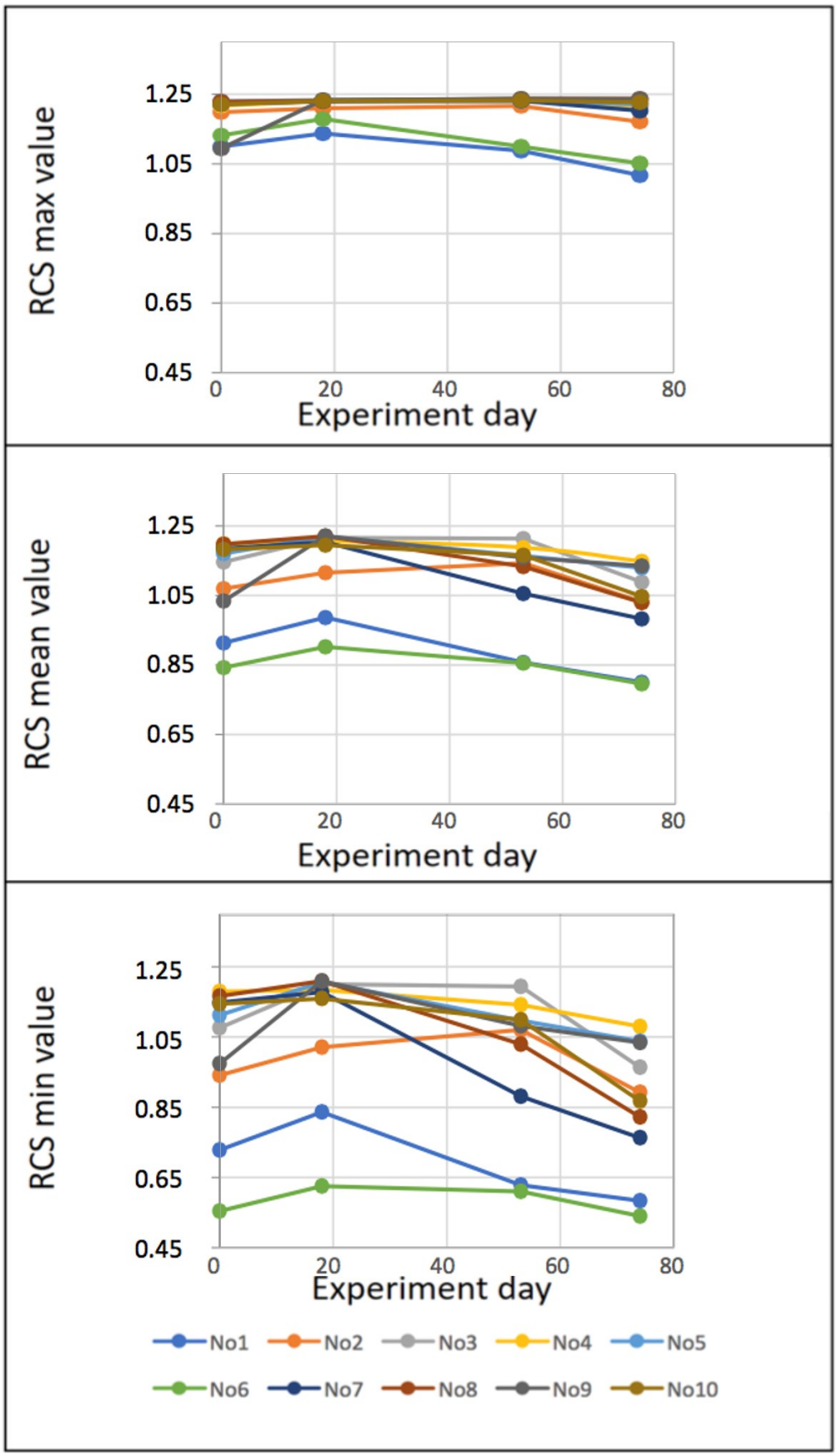

Figure 5-8 RCS maximum, mean and minimum values for the 10 palm tree trunks irradiated utilizing the L-band at separate times.

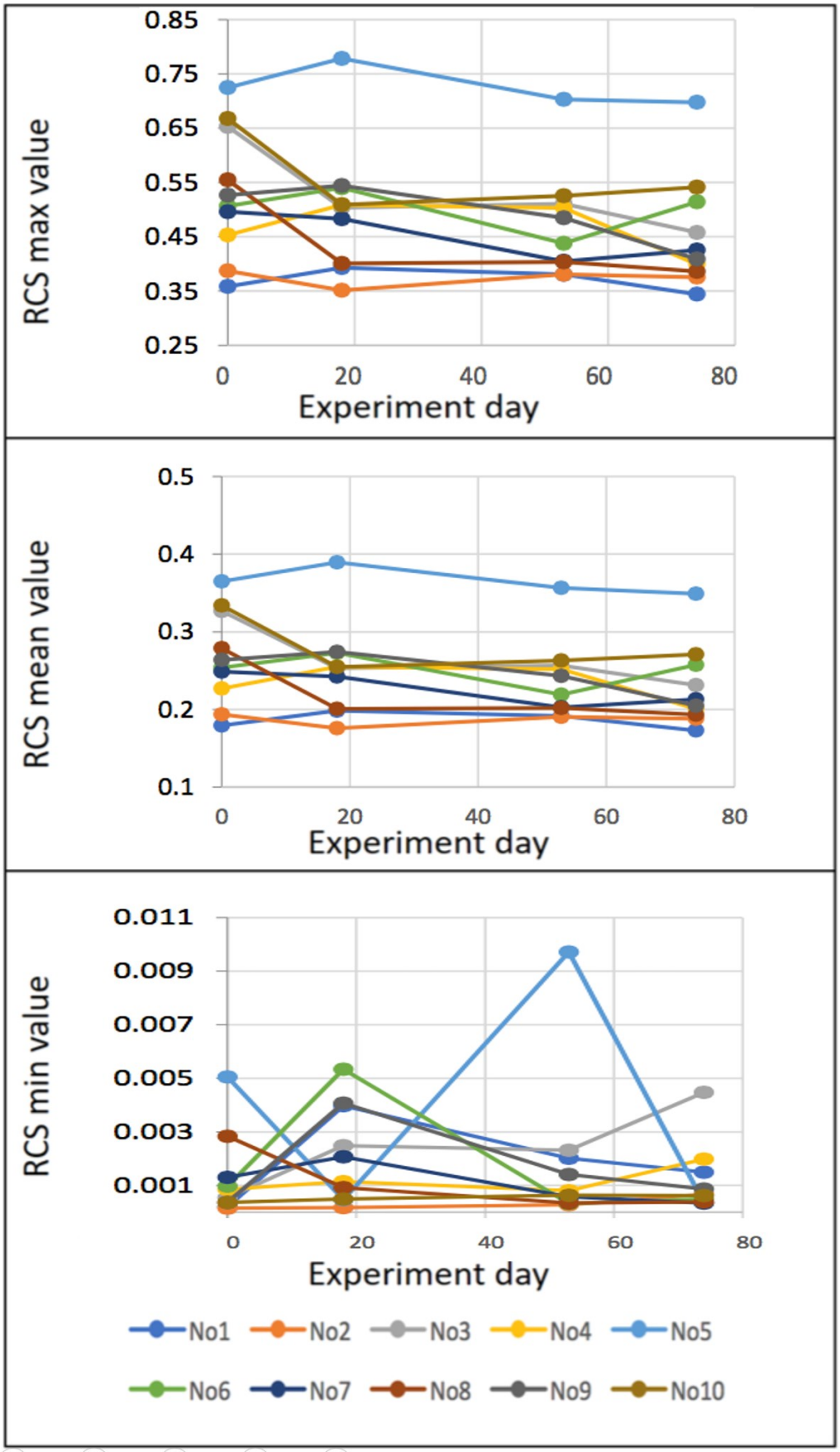

Figure 5-9 RCS maximum, mean and minimum values for the 10 palm tree trunks irradiated utilizing the X-band at separate times.

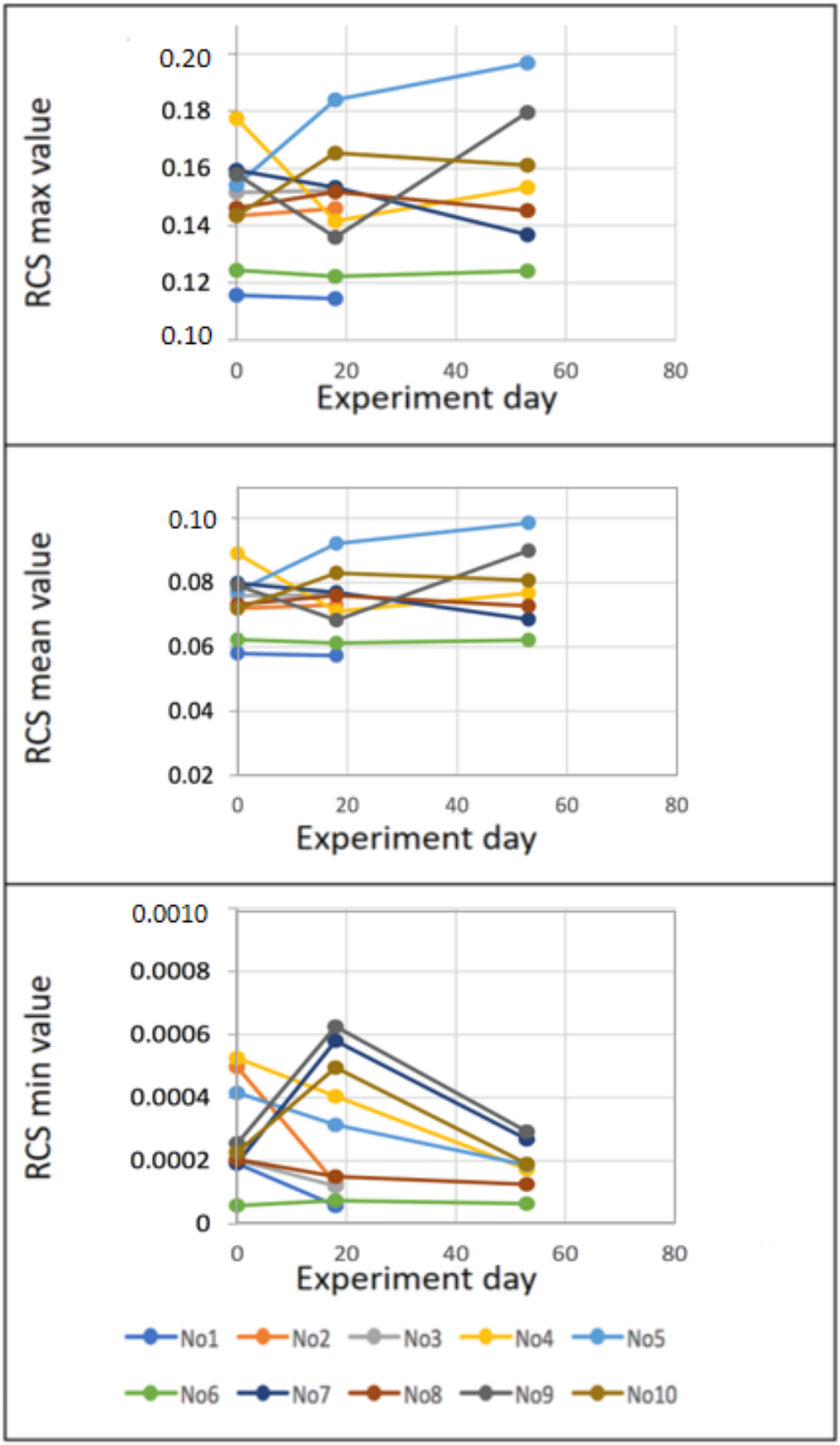

Figure 5-10 RCS maximum, mean and minimum values for the 10 palm tree trunks irradiated utilizing the Ku-band at separate times.

5-4.3 Comparison of measurement results over the experimental period

As seen in Figs. 5-9 and 5-10, regarding the measurement results for the X-band and Ku-band, all measurements were distinctively separated, and depicting a trend is difficult. Fig. 5-8 shows the results for L-band irradiation. From this, except for tree trunks No. 1 and No. 6, the maximum value is relatively the same, the minimum value decreases and the median value decreases slightly. Even when plotted in a graph showing the measurement results, the amplitude of the tree trunk measurements plotted in the graph moves downward over time. Therefore, it is clear that a relationship exists between the passage of time and the lower minimum value. Additionally, as previously discussed, the internal change caused by moisture loss and other factors was confirmed by monitoring the palm tree trunks' mass. Based on these two factors, a relationship was found for L-band measurement results: the backscattering minimum value decreases over time as the tree trunk loses its mass.

The reason for this phenomenon is that the mass loss in the various palm tree trunks does not occur equilaterally among all trees. Some trees may lose mass easily, while others may retain it for a more extended period. This results in unequal mass loss inside the palm tree trunks, causing multipath fading, and is possibly due to changes in fading variation and pattern, as shown in Fig. 5-11. Other reasons could be the biological changes that occur inside the palm tree trunks after they have been harvested, such as the destruction of tree cells and infection by bacteria or decay.

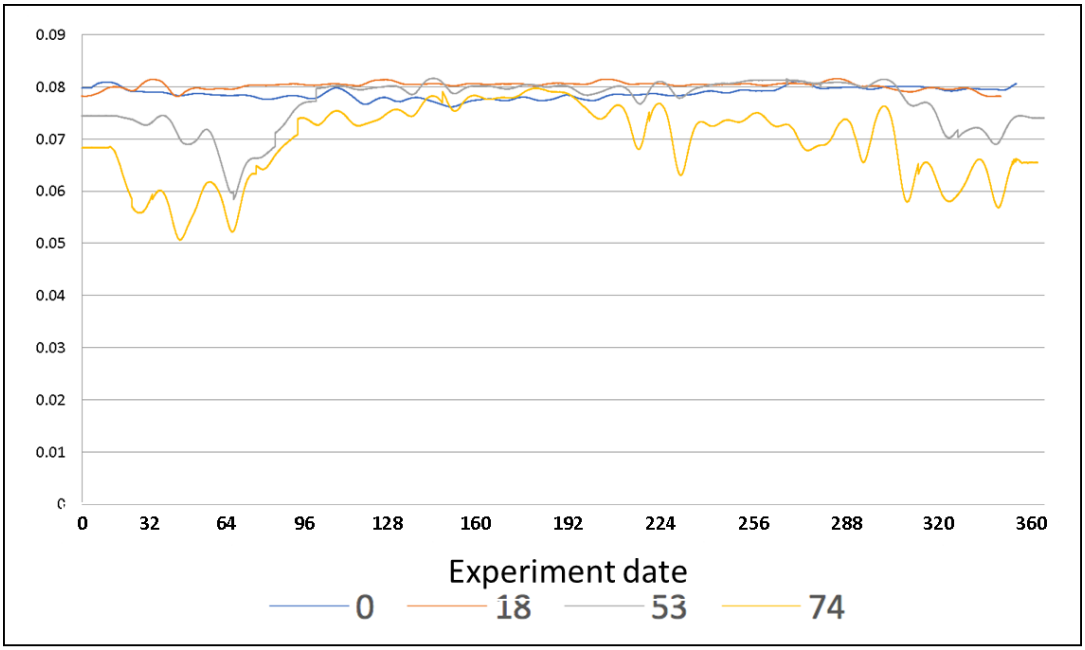

Figure 5-11 L-band measurement fading variation and pattern for tree No. 7 during a 360º rotation.

5-4.4 Histogram observations

To clarify the results, the results of measurements recorded utilizing each band are presented in histograms. Figs. 5-12, 5-13 and 5-14 show the histograms of palm tree trunks Nos. 7, 8 and 10 for the L-, X- and Ku-bands. From these results, almost no change in the histograms for the X-band and Ku-band can be seen over time in Figs. 5-13 and 5-14. A Gaussian distribution or Rayleigh distribution is always apparent; however, only the L-band shows a distinctive shape for all measurement results. As time passes, lower scattering increases. This L-band characteristic was also observed in the other palm tree trunks. Similar results are shown in Fig. 5-12.

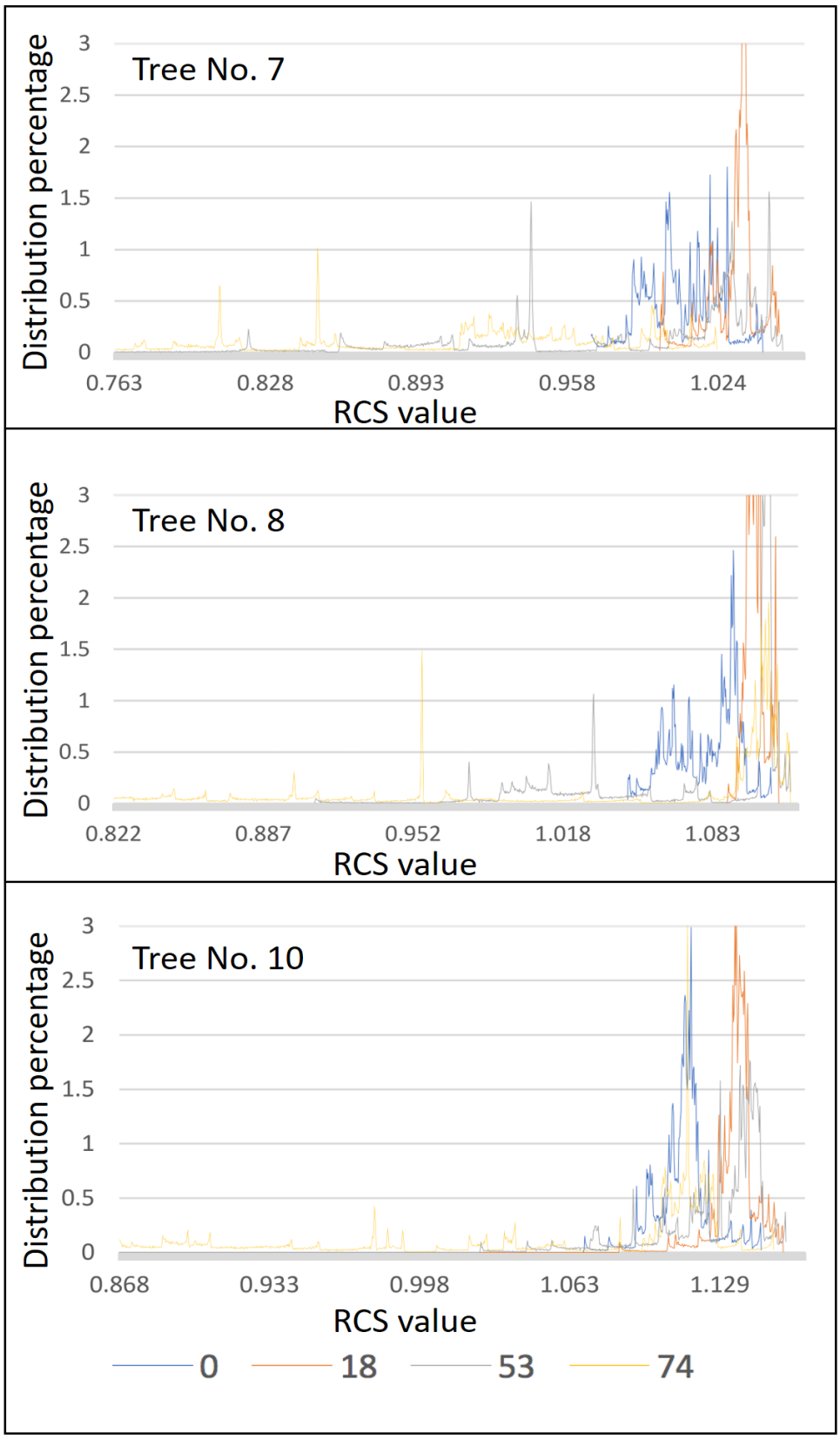

Figure 5-12 Histograms of tree trunk Nos. 7, 8 and 10 for the L-band.

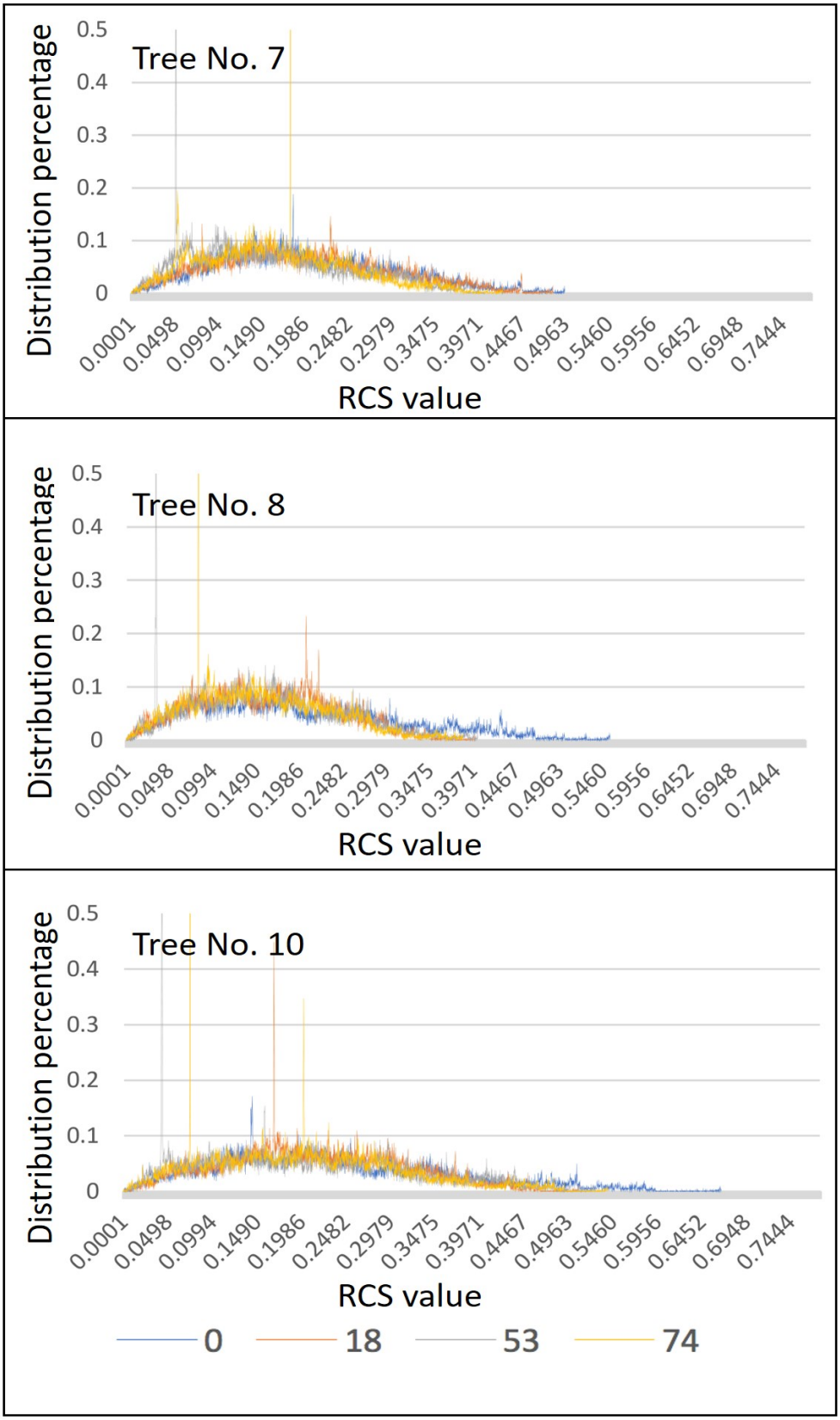

Figure 5-13 Histograms of tree trunk Nos. 7, 8 and 10 for the X-band.

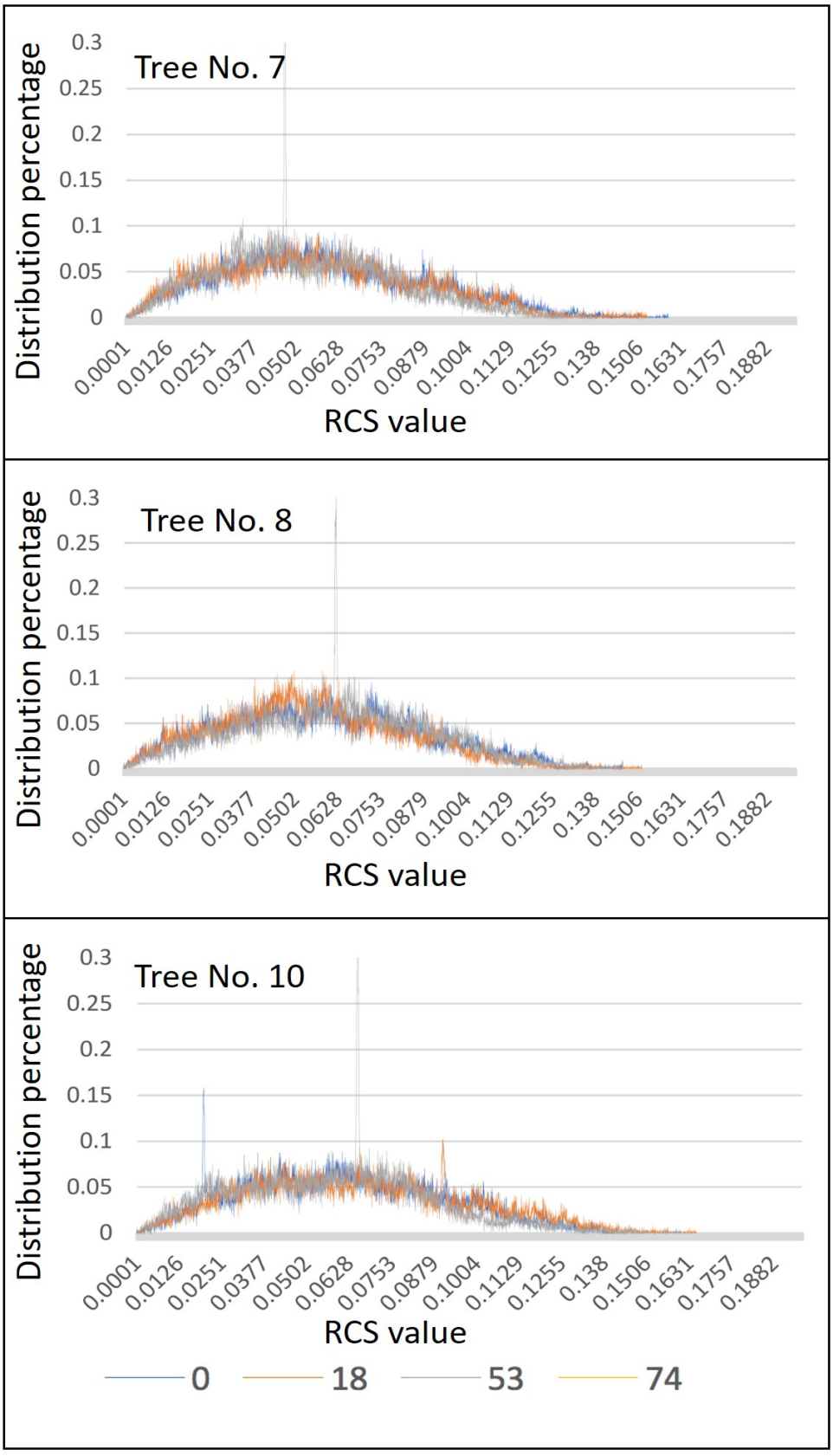

Figure 5-14 Histograms of tree trunk Nos. 7, 8 and 10 for the Ku-band.

CHAPTER 6 – DISCUSSION AND CONCLUSION

6-1 Discussion on Measurement of Water Content

6-1.1 Water Content in Foam Material

The purpose of this experiment was to measure the water content inside phenolic foam columns using microwave backscattering and applying the L-, X- and Ku-band frequencies. For this purpose, customized RCS measurement systems and an anechoic chamber were prepared, while a column of cylindrical foam was prepared as the target sample. For each water volume measured, water was carefully added to the column in the amount reported, and continuous measurements were made for the column's full circumference (360°). This is probably the first time that measurements have been taken applying such a method.

The experimental results show that, for all bands, the RCS mean value increased as the water content inside the column increased. Also, a change in the distribution of the RCS value with respect to the water content volume was observed. These results indicate the possibility of distinguishing differences in water content in phenolic foam columns using microwave backscattering.

Especially when using L-VV polarization, it is important to note that the difference could be distinguished even for the WTR25 and WTR50 cases. This is because many objects in the natural world contain a water-per-volume ratio of more than 50%. As the introduction mentioned, various fruits and vegetables have water content ratios greater than 50%. Similar species of trees include varieties in whose trunks the water content exceeds 50% per volume ratio. When pests infest such fruits or trees, their water content often declines to less than 25%. On the other hand, in a natural environment like a desert or dry agricultural soil in a field, the water content of the natural substance usually is less than 25%. Therefore, microwave backscattering of

the L-band can be used to observe the continuous change in the water content of trees or fruits. It can also be applied to the prevention of problematic agricultural issues such as pest infestation.

However, these conclusions stem from experimental results obtained under optimal conditions in an anechoic chamber. Additionally, in the L-band experiment, horizontal polarization (HH) was not measured. Furthermore, when selecting the object to be measured, more data collection is necessary using conditions such as various shapes and materials. In that case, the interference and analytical effects between the microwaves and object must also be considered. In addition, because substances that are present in nature comprise elements other than water, the study of experimental methods and evaluation methods is necessary to avoid these effects. Therefore, in the future, experiments must be carried out in a more realistic environment.

This experiment revealed a large fluctuation in the microwaves received, which seems to be due to the uneven dispersion of water content inside the column. The analysis of this variation using advanced statistics and pattern-matching technology applying artificial intelligence may enable further analysis, to a finer degree, of the moisture dispersed in the object. In the future, we will continue research based on this point.

6-1.1.1 Comparison with other water measurements

The dielectric constant and geometrical construction of the column material used in this experiment appears to be close to that of compressed snow or sand, as described in Section 4-2.1. Several studies have been conducted related to microwave reflections from various elements, such as soil, ice and snow [54][15][55][56]. Here,

we compare our experiment results with the results of a survey on reflections from snow, conducted by Ulaby and Dobson [30]. These researchers surveyed and collected data on radar backscattering in the field using various targets. Among the data they collected, the measurement of snow (wet and dry) using microwave backscattering bears some resemblance to our study, especially dry snow, which is mostly ice instead of free water, almost fully permeable to microwaves, and foam-like.

Table 6-1 A comparison of dry snow and wet snow backscattering coefficients, and the L-VV polarization results for our experiment. The first horizontal line is dry snow values, the second horizontal line is wet snow values, and the following lines are values from our experiment.

Band	Max	95 %ile	75 %ile	Median	25 %ile	5 %ile	Min	Mean	S.D.
L Dry 0°	12.9	11.2	8.3	6.2	3.8	-1.9	-7.2	5.7	4
L Wet 0°	15	12.3	9.7	7.2	4.1	-2.4	-6.8	6.7	4.4
L WTR0	-5.81	-6.43	-7.36	-8.08	-8.94	-9.83	-11.58	-8.13	1.01
L WTR25	-3.68	-4.13	-4.57	-5.50	-7.15	-10.51	-25.59	-6.23	2.41
L WTR35	-2.91	-3.06	-3.31	-3.85	-5.32	-6.83	-7.63	-4.34	1.26
L WTR50	-2.82	-2.95	-3.02	-3.14	-3.22	-3.38	-3.51	-3.13	0.13

(Backscattering coefficient: σ°)

Table 6-2 A comparison of dry snow and wet snow backscattering coefficients, and the X-VV polarization results for our experiment. The first horizontal line is dry snow values, the second horizontal line is wet snow values, and the following lines are values from our experiment.

Band	Max	95 %ile	75 %ile	Median	25 %ile	5 %ile	Min	Mean	S.D.
X Dry 0°	15.9	14.6	12.4	9.3	6.2	3.4	2	9.3	3.7
X Wet 0°	9.8	9.1	6.2	0	0	0	-5	2.8	3.7
X WTR0	8.82	7.62	6.33	5.07	3.65	-0.14	-20.72	4.67	2.38
X WTR25	13.34	12.71	11.34	10.22	8.14	2.16	-17.89	9.13	3.73
X WTR35	12.99	12.36	11.72	11.14	10.20	8.12	3.29	10.81	1.30
X WTR50	14.18	13.96	13.60	13.14	12.37	11.42	10.63	12.93	0.80

(Backscattering coefficient: σ°)

Table 6-3 A comparison of dry snow and wet snow backscattering coefficients, and the Ku-VV polarization results for our experiment. The first horizontal line is dry snow values, the second horizontal line is wet snow values, and the following lines are values from our experiment.

Band	Max	95 %ile	75 %ile	Median	25 %ile	5 %ile	Min	Mean	S.D.
Ku Dry 0°	18.7	16.3	12.8	10.7	8	3.4	1.1	10.3	3.8
Ku Wet 0°	14.8	14.2	12.7	10.2	3.3	0	-1.2	8.5	5
Ku WTR0	7.65	6.26	5.00	3.90	2.19	-1.18	-18.71	3.35	2.41
Ku WTR25	14.77	13.71	12.47	11.45	9.30	5.81	-8.32	10.70	2.51
Ku WTR35	14.75	14.28	13.52	12.79	11.18	8.72	3.39	12.22	1.79
Ku WTR50	15.47	15.02	14.68	14.14	13.64	12.63	10.38	14.05	0.79

(Backscattering coefficient: σ°)

Tables 6-1, 6-2 and 6-3 show the descriptive statistics of backscatter coefficients that Ulaby and Dobson surveyed, and the descriptive statistics from our study for L-VV, X-VV, and Ku-VV, respectively. It is worth noting that the descriptive statistics from Ulaby and Dobson's survey and those from the present study have a statistically different aspect. Each "data point" in Ulaby and Dobson's survey is a backscatter coefficient shown in their survey and is a representative value in and of itself. Thus, for instance, the mean shown in Ulaby and Dobson's survey is the "mean of means," and the standard deviation shown may be a value close to the standard error rather than the standard deviation. On the other hand, the descriptive statistics shown in the tables of the present study are derived from single measurements, and the mean (or median) stands as one representative value. In this sense, Ulaby and Dobson's descriptive statistics may be considered a "possible range of backscatter coefficient means, or representative values."

A rough estimation of the possible L-VV backscatter coefficient range, for instance a 99% confidence interval, based on the mean and standard deviation for wet and dry snow would be -3.60 to 15.00 dB for dry snow and -3.53 to 16.93 dB for wet snow.

The average backscatter coefficients from our measurements were mostly outside the above ranges as well, except for those of WTR50. The difference between dry snow and wet snow shown in Ulaby and Dobson's survey was around 1 dB, which is relatively small and makes the types of snow difficult to distinguish from each other. The same applies to our observation, which exhibits a difference of about 2 dB between water conditions. Instead, the standard deviation from our observed data (note, again, that Ulaby and Dobson's standard deviation should be assumed to be a standard error of the mean) is largely different between water content conditions. As described earlier, standard deviation along with the average of the measured data may be a useful index for estimating a column's water content.

In comparing X-VV polarization, most of the mean backscatter coefficients from our observations are not in the "possible range of backscatter coefficient mean" for wet snow. On the other hand, mean backscatter coefficients for the conditions of WTR25 to WTR50 measured using Ku-VV were in the range of possible mean backscatter coefficients.

6-1.1.2 Discussion of microwave wavelength and target object size

As shown in Fig. 4-1, this experiment used a column made of phenolic foam having a diameter of 20 cm and a height of 75 cm. Additionally, as shown in Fig. 4-3, the column was placed on the rotating table and a RCS measurement system was positioned 2.9 m from the column in the horizontal direction. The wavelength of the L-band RCS measurement system that this experiment used was about 23.5 cm; this value is close to the column's diameter. In such a case, it is conceivable that a complicated interference exists in the measurement results due to the Mie scattering or diffraction effect that Chapter 2 described. However, this experiment measures

only the backscattering components of the enormous number of reflection points scattered in the column. This measurement was taken in an anechoic chamber. Therefore, the influence of forward scattering, such as Mie scattering or a diffraction effect, can be ignored.

6-1.1.3 Comparison of column water contents and microwave backscattering

In Fig. 6-1, the distribution of RCS values for the L-VV, X-VV and Ku-VV polarizations is shown as a box and whisker chart. In this figure, the bottom whisker indicates the 5th percentile, while the top whisker indicates the 95th percentile. Additionally, the bottom of the box is the 25th percentile, the top of the box is the 75th percentile and the line segment in the box is the median (50th percentile).

Paying attention to the position of the interquartile range (IQR), one can see that it moves upward in the order of WTR0, WTR25, WTR35, and WTR50. Therefore, when a sufficient number of measured values is obtained, as in this experiment, the fact becomes clear that backscattering increases in any band as the internal water content increases.

Next, even with a comparison using the 5th and 95th percentile whiskers that are more stringent than the IQR, the bottom whiskers of WTR50 are located above the top whiskers of WTR0 for all three bands. This comparison shows that the data distributions of the WTR50 and WTR0 columns can be distinguished from each other for all bands. Notably, for the L-VV band, as shown in Fig. 6-1 (A), the bottom whisker of WTR50 is higher than the top whisker of WTR25. Therefore, in L-VV, distinguishing between WTR50 and WTR25 is possible.

Finally, for all bands, variations in the dispersion range width should be noticed. From WTR0 to WTR25, the dispersion range width expanded rapidly. This is considered to be the effect of unevenness in the distribution of reflection points when the reflection point increases as the amount of water penetrating the column increases. In WTR25 to WTR35, although the number of reflection points increases, because the unevenness of distribution is maintained, it is believed the median value moves upward while maintaining the dispersion range width. In WTR35 to WTR50, the uneven distribution began decreasing due to an increase in the column's reflection point. The width of variance also began converging. Particularly, for L-VV, the distribution unevenness of the reflection points for WTR50 was nearly gone, and it is believed that dispersion became very narrow.

These results clearly show that distinguishing differences in water content using microwave backscattering is possible.

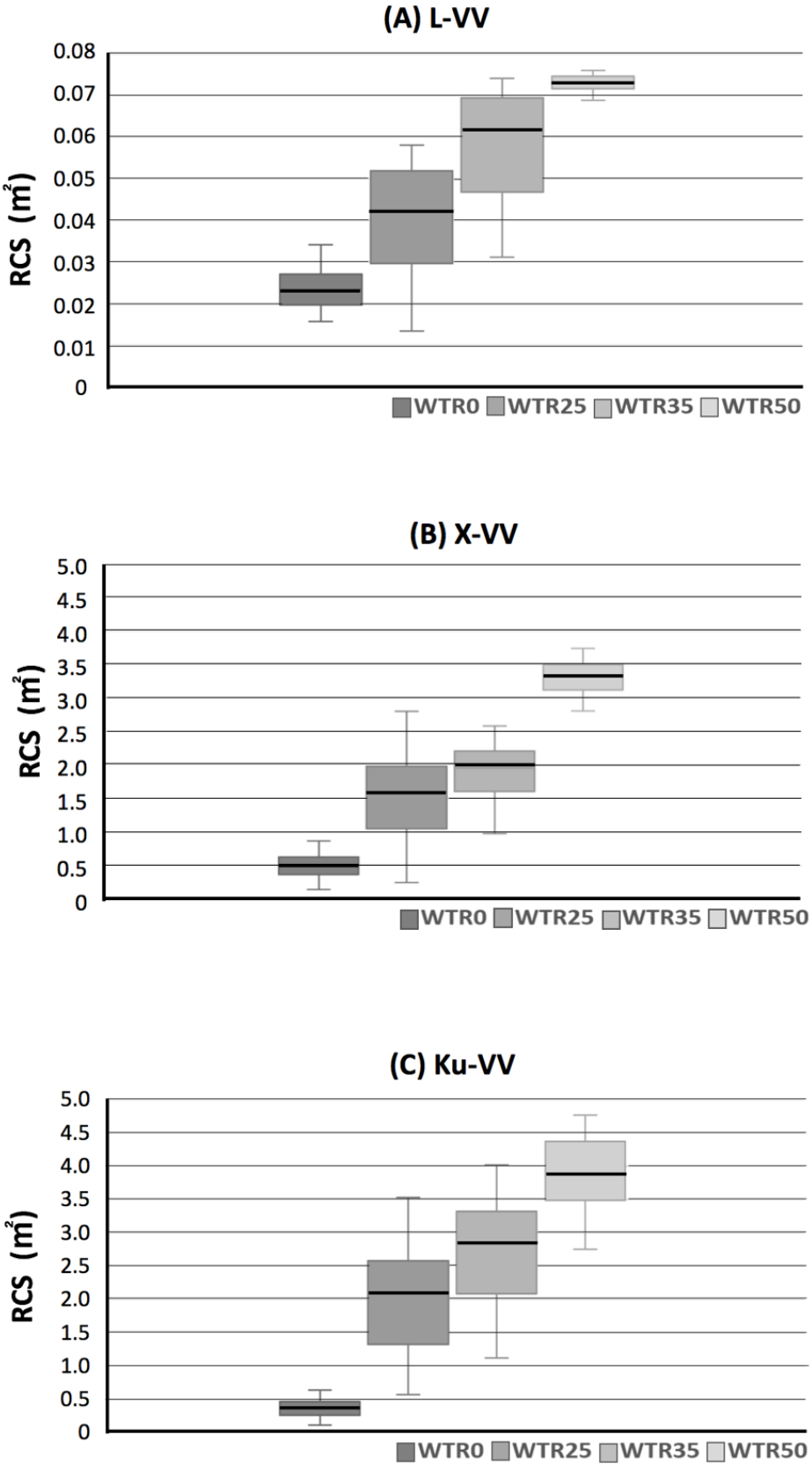

Figure 6-1 Box whisker charts for the distribution of RCS values obtained using L-VV, X-VV, and Ku-VV polarization.

6-2 Water Content in Palm Tree Trunks

Following the successful measurements, analyses, and results of the previous experiment, this experiment was conducted to test the applicability of utilizing only microwave backscattering measurements to determine changes in the water content volume of actual plants (i.e., palm trees) over a period of time. The experiment found that, for the X-band and Ku-band, determining a change in palm tree trunks' internal structure is difficult. Based on the characteristic measurement results obtained by applying the short-wavelength X-band and Ku-band, in terms of the scattering properties of the tree trunk surfaces, the conclusion was that the sago palm tree is covered by a thick epidermis (i.e., hard bark).

However, the results of the L-band measurements presented interesting possibilities. Irradiating the palm tree trunks with L-band microwaves, or possibly even lower frequencies, enabled the observation of changes inside the tree trunk, including even the thick-barked sago palm trees that this experiment used. Importantly, as done in this experiment, the utilization of histograms rather than numerical values appears to be a practical method for recognizing a pattern or patterns. This concept will become more viable as advancements are made in the rapidly developing area of pattern recognition technology.

The purpose of this dissertation was to prove that the water content in palm trees can be determined utilizing only microwave backscattering measurements and by analyzing the results. This was achieved by showing the relationship between the direct microwave backscattering results obtained utilizing the L-band and the loss of mass in the palm tree trunks measured. This relationship is assumed to be a characteristic trait based on the basic properties of microwaves and the ways in which they react when they come into contact with a bipolar molecular structure.

However, the explanation for the change in multipath fading is only an assumption. In the graphs plotted using the number of days elapsed and the mean values (Fig. 5-8), numerous instances show a sudden change in the latter half of the measurements taken. This may be related to a change other than moisture loss, e.g., destruction of tree cells, decay, etc. Future studies must clarify this issue by increasing the accuracy of the measurements taken.

Additionally, this study was the first attempt to display a large amount of data utilizing multipath fading in a histogram. Therefore, it may be possible to determine the internal structure of tree trunks in detail by improving the pattern analysis method. For future research, the investigation of new methods of analysis is desirable.

6-3 Conclusion

In this dissertation, the author purpose was to prove that the differences in water content in vegetation such as palm trees can be determined using only an analysis of the microwave backscattering measured from the object. The backscattered microwaves were recorded by RCS measurement systems developed with specifications that enabled high speed, remote measurement.

From the result of the first experiment, it was proven that differences in the water content of foam cylinders prepared with varying volumes of water can be distinguished by all the three frequency bands. The conducted experiment is very unique, and the obtained results will help further studies regarding active microwave remote sensing of water content.

The success of this experiment motivates us to use actual palm tree trunks, and an experimental regime representing the phenomenon of the trees being gradually depleted of water over a period of time was used. A similar method of irradiating the

tree trunks with the three microwave frequencies, measuring the microwaves backscattered, and the ensuing analysis of the recorded results proved that microwave backscattering can be used to remotely measure the water content in objects more specifically, palm trees and thus, determine changing conditions in tree health.

Also, it was found that the X-band and Ku-band frequencies, with shorter wavelengths, are not capable of penetrating harder skinned vegetation like the sago palm used for this study. However, they can be used to determine distance and external characteristics. Still, the L-band was able to penetrate the object, reflect off the bipolar molecular structures (i.e., water) and provide a backscattering intensity sufficient for determining the water content level.

Therefore, it has been concluded that the objective of this experiment in this study to measure and monitor the state of change in palm trees using only microwave backscattering was achieved. Also, this measurement method is new, and it could add a new approach to measuring moisture content and palm tree conditions noninvasively.

Of course, as witnessed in the results analysis, the backscattering intensity is larger in parallel with higher water content. Even so, using the method presented in both experiments, the detection of water content of objects containing 25% and even lower, 0%, was still possible. In a natural environment, especially in arid regions, the water content per volume is often below 25%. Furthermore, in daily surroundings, (i.e., the dry wood used in construction), the water content is approximately 6 to 10% (converted to volume ratio). The water content of fields, relatively dry soil and the like is also often below 25%. Accordingly, it is presumed that, using the L-band wavelength, water content conditions can be distinguished among objects utilizing only microwave backscattering.

6-4 Future Work

The conclusions are derived from experimental results obtained under only the best possible measurement conditions, in an anechoic chamber without interference and under controlled climatic conditions. In the future, experiments in a more realistic environment are required. Furthermore, in selecting objects to be measured, it is necessary to add more data by repeating the experiment using various shapes and materials. This experiment found that statistical and probabilistic analysis and pattern matching technology to estimate the similarity of results is important for fading analysis. However, knowledge of this matter is minimal at present. In recent years, the use of artificial intelligence to conduct such a signal analysis has begun. Although this is still an unknown area and is in the early stages of development, considering the success achieved in other areas, hope exists that a new methodology will be created for data analysis in remote sensing.

The author's future goal is to study the water content conditions of actual date palm trees and related characteristics. Because date palm trees contain more water in their trunks as compared to other tree species, date palm tree trunks with different water content levels will be tested to determine the possibility of using microwaves to monitor tree health conditions. Additionally, a method of monitoring palm trees individually from different angles will be investigated. If the experiment succeeds in distinguishing between different water content levels, combining the use of RCS measurement systems in agriculture will be beneficial in terms of monitoring the health of vegetation and agriculture products.

BIBLIOGRAPHY

[1] A. Menzel, T. H. Sparks, N. Esrella, and E. Bissolli, "European phenological response to climate change matches the warming pattern," *Glob. Chang. Biol.*, vol. 12, no. 10, pp. 1969–1976, 2006.

[2] J. Kim, "Could Climate Change Drive Giant Pandas to Extinction?," *Time Magazine*, Nov-2012.

[3] M. B. K. Darkoh, "DESERTIFICATION IN AFRICA," *J. East. Afr. Res. Dev.*, vol. 19, pp. 1–50, 1989.

[4] L. El-Juhany, "Degradation of date palm trees and date production in Arab countries: causes and potential rehabilitation," *Aust. J. Basic Appl. Sci.*, vol. 4, no. 8, pp. 3998–4010, 2010.

[5] S. Murphy and B. Briscoe, "The red palm weevil as an alien invasive: Biology and the prospects for biological control as a component of IPM," *Biocontrol News Inf.*, vol. 20, no. 1, pp. 35–46, 1999.

[6] J. . Faleiro, "A review of the issues and management of the red palm weevil Rhynchophorus ferrugineus (Coleoptera: Rhynchophoridae) in coconut and date palm during the last one hundred years," *Int. J. Trop. Insect Sci.*, vol. 26, no. 3, pp. 135–154, 2006.

[7] E.-F. Mozib, "Effect of red palm weevil, Rhynchophorus ferrugineus (Olivier) infestation on temperature profiles of date palm tree," *J. Entomol. Nematol.*, vol. 5, no. 6, pp. 77–83, 2013.

[8] F. Algneaer, S. Sakai, H. Nohmi, and A. Nohmi, "A Study on Date Palm Trees Using Airborne SAR in Saudi Arabia," *Proc. 52nd spring Conf. Remote Sens. Soc. Japan*, pp. 59–62, 2012.

[9] J. V. G. A. Durnin and J. Womersley, "Body fat assessed from total body density and its estimation from skinfold thickness: measurements on 481 men and women aged from 16 to 72 years," *Br. J. Nutr.*, vol. 32, no. 1, pp. 77–97, 1973.

[10] R. Shamanna, *Handbook of analysis and quality control for fruit and vegetable products*. Tata McGraw-Hill Education, 1986.

[11] H. Yoshimatsu and S. Abe, "A review of landslide hazards in Japan and assessment of their susceptibility using an analytical hierarchic process (AHP) method," *Landslides*, vol. 3, no. 2, pp. 149–158, 2006.

[12] J. Soria-Ruiz, Y. Fernandez-Ordonez, H. McNairm, and J. Bugden-Storie, "Corn monitoring and crop yield using optical and RADARSAT-2 images," *Int. Geosci. Remote Sens. Symp. IGARSS*, pp. 3655–3658, 2007.

[13] Y. Jiang and Y. Zhang, "Research on Microwave Measurement for Grain Moisture Content in Granary," *2009 IITA Int. Conf. Control. Autom. Syst. Eng. (case 2009)*, pp. 327–330, 2009.

[14] H. Messer and O. Sendik, "A New Approach to Precipitation Monitoring," *IEEE Signal Process. Mag.*, vol. 32, no. 3, pp. 110–122, 2015.

[15] F. Ulaby and P. Batlivala, "Optimum Radar Parameters for Mapping Soil Moisture," *IEEE Trans. Geosci. Electron.*, vol. 14, no. 2, pp. 81–93, 1976.

[16] H. Vernieuwe, N. E. C. Verhoest, H. Lievens, and B. De Baets, "Possibilistic soil roughness identification for uncertainty reduction on SAR-retrieved soil moisture," *IEEE Trans. Geosci. Remote Sens.*, vol. 49, no. 2, pp. 628–638, 2011.

[17] S. Frolking, S. Hagen, T. Milliman, M. Palace, J. Z. Shimbo, and M. Fahnestock, “Detection of Large-Scale Forest Canopy Change in Pan-Tropical Humid Forests 2000–2009 With the SeaWinds Ku-Band Scatterometer,” *IEEE Trans. Geosci. Remote Sens.*, vol. 50, no. 7, pp. 2603–2617, Jul. 2012.
[18] S. E. Nicholson, “Application of Remote Sensing to Climatic and Environmental Arid and Semi-Arid Lands,” *Geosci. Remote Sens. Symp.*, vol. 3, no. C, pp. 985–987, 2001.
[19] M. Kehat, “Threat to Date Palms in Israel , Jordan and the Palestinian Authority by the Red,” *Phytoparasitica*, vol. 27, pp. 241–242, 1999.
[20] M. S. Venkatesh and G. S. V Raghavan, “An overview of microwave processing and dielectric properties of agri-food materials,” *Biosyst. Eng.*, vol. 88, no. 1, pp. 1–18, 2004.
[21] V. V Lisovsky, “Automatic control of moisture in agricultural products by methods of microwave aquametry,” *Meas. Sci. Technol.*, vol. 18, no. 4, pp. 1016–1021, 2007.
[22] S. Trabelsi and S. O. Nelson, “Microwave Sensing of Quality Attributes of Agricultural and Food Products,” *IEEE Instrum. Meas. Mag.*, vol. 19, no. 1, pp. 36–41, 2016.
[23] A. W. Kraszewski, S. Trabelsi, and S. O. Nelson, “Simple Grain Moisture Content Determination from Microwave Measurements,” *Am. Soc. Agric. Eng.*, vol. 41, no. 1, pp. 129–134, 1998.
[24] T. Jayanthi, B. S. Navya, and K. Vanitha, “Microwave Moisture Measurement Technique In Industrial Application,” *Int. J. Electr. Electron. Commun. Eng.*, vol. 1, no. 1, pp. 14–18, 2015.
[25] Y. Jiang and Y. Zhang, “Research on microwave measurement for grain moisture content in granary,” in *2009 IITA International Conference on Control, Automation and Systems Engineering*, 2009, pp. 327–330.
[26] H. M. A. Al-Mattarneh, D. K. Ghodgaonkar, and W. M. B. W. A. Majid, “Microwave nondestructive testing for classification of Malaysian timber using free-space techniques,” *6th Int. Symp. Signal Process. Its Appl.*, vol. 2, pp. 450–453, 2001.
[27] R. Lucas *et al.*, “An evaluation of the ALOS PALSAR L-band backscatter - Above ground biomass relationship Queensland, Australia: Impacts of surface moisture condition and vegetation structure,” *IEEE J. Sel. Top. Appl. Earth Obs. Remote Sens.*, vol. 3, no. 4 PART 2, pp. 576–593, 2010.
[28] M. El Hajj *et al.*, “Soil Moisture Retrieval Over Irrigated Grasslands Using X-Band Sar Data,” pp. 1328–1331, 2015.
[29] I. Mladenova, V. Lakshmi, J. P. Walker, D. G. Long, and R. De Jeu, “An assessment of QuikSCAT ku-band scatterometer data for soil moisture sensitivity,” *IEEE Geosci. Remote Sens. Lett.*, vol. 6, no. 4, pp. 640–643, 2009.
[30] F. T. Ulaby and M. C. Dobson, *Handbook of Radar Scattering Statistics for Terrain*. Artech House, 1989.
[31] M. S. Venkatesh and G. S. V Raghavan, “An overview of dielectric properties measuring techniques,” *Can. Biosyst. Eng. / Le Genie des Biosyst. au Canada*, vol. 47, 2005.
[32] U. Kaatze and C. Hübner, “Electromagnetic techniques for moisture content determination of materials,” *Meas. Sci. Technol.*, vol. 21, no. 8, p. 82001, 2010.
[33] C. Vallejos and W. Grote, “Wood moisture content measurement at 2.45 GHz,” *SBMO/IEEE MTT-S Int. Microw. Optoelectron. Conf. Proc.*, pp. 221–225, 2009.

[34] S. J. Zegelin, I. White, and D. R. Jenkins, “Improved field probes for soil water content and electrical conductivity measurement using time domain reflectometry,” *Water Resour. Res.*, vol. 25, no. 11, pp. 2367–2376, 1989.
[35] T. Saito *et al.*, “Monitoring of Stem Water Content of Native and Invasive Trees in Arid Environments Using GS3 Soil Moisture Sensors,” *Vadose Zo. J.*, vol. 15, no. 3, pp. 1–9, 2016.
[36] S. Gharechelou, R. Tateishi, J. Tetuko, and S. Sumantyo, “Interrelationship Analysis of L-Band Backscattering Intensity and Soil Dielectric Constant for Soil Moisture Retrieval Using PALSAR Data,” *Adv. Remote Sens.*, no. March, pp. 15–24, 2015.
[37] J. M. Blonquist, S. B. Jones, and D. A. Robinson, “Standardizing Characterization of Electromagnetic Water Content Sensors,” *Vadose Zo. J.*, vol. 4, no. 4, pp. 1059–1069, 2005.
[38] U. Kaatze, “Techniques for measuring the microwave dielectric properties of materials,” *Metrologia*, vol. 47, no. 2, pp. S91–S113, 2010.
[39] C. F. Bohren and D. R. Huffman, *Absorption and scattering of light by small particles*. John Wiley & Sons, 2008.
[40] C. G. Koops, “On the Dispersion of Resistivity and Dielectric Constant of Some Semiconductors at Audiofrequencies,” *Phys. Rev.*, vol. 83, p. 121, 1951.
[41] T. Peter, *Introduction to radar target recognition*. IET, 2005.
[42] C. John C and M. Ropert N, *Synthetic Aperture Radar*. New York: John Wiely & Sons, 1991.
[43] R. Sabine, *Real-time Processing of Ground-Based Synthetic Aperture Radar (GB-SAR) Measurements*. Technische Universität Darmstadt, 2011.
[44] Agilent Technologies Inc., “Agilent Network Analyzer Basics,” 2004.
[45] V. N. Bringi and V. Chandrasekar, *Polarimetric Doppler weather radar: principles and applications*. Cambridge University Press, 2001.
[46] G. Mokhtari, Q. Zhang, C. Hargrave, and J. C. Ralston, “Non-Wearable UWB Sensor for Human Identification in Smart Home,” *IEEE Sens. J.*, vol. 17, no. 11, pp. 3332–3340, 2017.
[47] A. G. Yarovoy, L. P. Ligthart, J. Matuzas, and B. Levitas, “UWB radar for human being detection,” *IEEE Aerosp. Electron. Syst. Mag.*, vol. 21, no. 11, pp. 22–26, 2006.
[48] J. Li, Z. Zeng, J. Sun, and F. Liu, “Through-wall detection of human being’s movement by UWB radar,” *IEEE Geosci. Remote Sens. Lett.*, vol. 9, no. 6, pp. 1079–1083, 2012.
[49] A. W. Kraszewski and S. O. Nelson, “Application of microwave techniques in agricultural research,” *Microw. Optoelectron. Conf. Proceedings., 1995 SBMO/IEEE MTT-S Int.*, vol. 1, pp. 117–126, 1995.
[50] M. Moghaddam and S. S. Saatchi, “Monitoring tree moisture using an estimation algorithm applied to SAR data from BOREAS,” *IEEE Trans. Geosci. Remote Sens.*, vol. 37, no. 2, pp. 901–916, 1999.
[51] J. Škramlik, M. Novotny, and K. Šuhajda, “Interaction of microwave radiation with wet porous material,” in *International Workshop of NDT Experts*, 2011, vol. 0, no. 2, pp. 10–12.
[52] S. Okamura, “Microwave technology for moisture measurement,” *Subsurf. Sens. Technol. Appl.*, vol. 1, no. 2, pp. 205–227, 2000.
[53] H. HIROSAWA, “Radar backscatters from vegetation; a review of a laboratory-based measurement technique,” in *Geoscience and Remote Sensing Symposium*, 1991, vol. 3, pp. 1519–1522.

[54] T. J. Schmugge, “Remote Sensing of Soil Moisture: Recent Advances,” *IEEE Trans. Geosci. Remote Sens.*, vol. GE-21, no. 3, pp. 336–344, 1983.
[55] F. T. Ulaby, “Radar measurement of soil moisture content,” *Antennas Propagation, IEEE Trans.*, vol. 22, no. 2, pp. 257–265, 1974.
[56] F. T. Ulaby, W. H. Stiles, L. F. Dellwig, and B. C. Hanson, “Experiments on the Radar Backscatter of Snow,” *IEEE Trans. Geosci. Electron.*, vol. 15, no. 4, pp. 185–189, 1977.
[57] F. Algneaer, M. Suganuma, S. Iwata, S. Sakai, H. Nohmi, and A. Nohmi, “Application of Microwave Backscattering to Monitor the State of Change in Truncated Palm Trees,” *Int. J. Geol. Earth Sci.*, vol. 3, no. 2, pp. 10–25, 2017.
[58] F. Algneaer, S. Sakai, and H. Nohmi, “MEASUREMENT STUDY ON PALM TREES BY USING DIFFERENT FREQUENCY BANDS Fahad Algneaer , Shigekazu Sakai , Hitoshi Nohmi,” *IEEE Geosci. Remote Sens. Symp.*, pp. 4094–4097, 2014.

LIST OF ACADEMIC ACHIEVEMENTS

Category	
Articles in refereed journals	○ F. Algneaer, M. Suganuma, S. Iwata, S. Sakai, H. Nohmi, and A. Nohmi, "Application of Microwave Backscattering to Monitor the State of Change in Truncated Palm Trees," *Int. J. Geol. Earth Sci.*, vol. 3, no. 2, pp. 10–25, 2017.
38巻2号掲載予定	○ F. Algneaer, M. Suganuma, S. Iwata, S. Sakai, H. Nohmi, and A. Nohmi, "A Fundamental Study on the Characteristics of Microwave Back Scattering – Using Backscattering to Compare Water Content in a Solid Object," Journal of Remote Sensing Society of Japan. (Yet to be published)
Presentations at International conferences	F. Algneaer, M. Suganuma, S. Iwata, S. Sakai, H. Nohmi, "A Study of Radar Backscattering to Estimate Moisture Content," International Remote Sensing Conference 2016, KACST, pp. 67. F. Algneaer, S. Sakai, and H. Nohmi, "MEASUREMENT STUDY ON PALM TREES BY USING DIFFERENT FREQUENCY BANDS Fahad Algneaer, Shigekazu Sakai , Hitoshi Nohmi," in *IEEE Geoscience and Remote Sensing Symposium*, 2014, pp. 4094–4097.
Presentations at domestic conferences	F. Algneaer, M. Suganuma, S. Iwata, S. Sakai, H. Nohmi, "Fundamental Study of Moisture Content Estimation by Radar Backscattering". Japan Society of Photogrammetry and Remote Sensing, 2015, 平成27年度秋季学術講演会予稿集 pp. 47-50 F. Algneaer, S. Sakai, H. Nohmi, and A. Nohmi, "A Study on Date Palm Trees Using Airborne SAR in Saudi Arabia," in *Proceedings of the 52nd spring conference of the Remote Sensing Society of Japan*, 2012, pp. 59–62.